



Metals in coarse ambient aerosol as markers for source apportionment and their health risk assessment over an eastern coastal urban atmosphere in India

Upasana Panda · R. Boopathy · H. S. Gadhavi · K. Renuka · Sachin S. Gunthe · Trupti Das

Received: 19 May 2020 / Accepted: 5 April 2021 / Published online: 29 April 2021
© The Author(s), under exclusive licence to Springer Nature Switzerland AG 2021

Abstract Ambient PM₁₀ (particulate matter with aerodynamic diameter $\leq 10 \mu\text{m}$) samples were collected and characterized from July 2012 to August 2013 with the objective to evaluate the variation in elemental concentration and use the same as markers for source apportionment and health risk assessment for the first time over Bhubaneswar, India. The yearly average mass of PM₁₀ was $82.28 \mu\text{g}/\text{m}^3$, which

was ~37% higher than the national ambient air quality (NAAQ) standards. Maximum PM₁₀ concentration was observed during winter season followed by post-monsoon, pre-monsoon, and monsoon months. Acid soluble components in the PM₁₀ samples were analyzed using ICP-OES (inductive coupled plasma optical emission spectroscopy), and 19 different elements including heavy metals were determined. Enrichment factor analysis attributed the source to either crustal or non-crustal origin. Principal component analysis (PCA) revealed that crustal sources, industrial activities, and vehicular emissions were significant contributors to PM mass. The contribution of total average elemental concentration showed a seasonal variation with the lowest ($11.96 \mu\text{g}/\text{m}^3$) and highest ($17.77 \mu\text{g}/\text{m}^3$) during monsoon and winter, respectively, which is relatively less significant than the variation in total PM₁₀ mass that ranged between $48.43 \mu\text{g}/\text{m}^3$ in monsoon and $138.24 \mu\text{g}/\text{m}^3$ during the winter season. This observation evidences the predominant contribution of local/regional emission sources to the metallic components in coarse PM₁₀ mass, which is corroborated by the wind pattern studies carried out using polar plots and a Lagrangian Particle Dispersion Model (LPDM) FLEXPART. Further, carcinogenic and non-carcinogenic health risk assessments of the measured elements that find their way into the human body through different exposure pathways have been calculated using United State Environmental Protection Agency (USEPA) standards. The carcinogenic risk of most of the elements was insignificant. The

Supplementary information The online version contains supplementary material available at <https://doi.org/10.1007/s10661-021-09057-3>.

U. Panda · R. Boopathy · T. Das
Environment and Sustainability Department, CSIR-
Institute of Minerals and Materials Technology,
Bhubaneswar 751013, India

U. Panda · R. Boopathy · T. Das (✉)
Academy of Scientific and Innovative Research (AcSIR),
Ghaziabad 201002, India
e-mail: truptiimmt@gmail.com; truptidas@immt.res.in

H. S. Gadhavi · K. Renuka
Space and Atmospheric Science Division, Physical
Research laboratory (PRL), Ahmadabad, Gujarat, India

S. S. Gunthe
EWRE Division, Dept. of Civil Engineering, Indian
Institute of Technology Madras, Chennai-36, Tamil Nadu,
India

S. S. Gunthe
Laboratory for Atmospheric and Climate Sciences, Indian
Institute of Technology Madras, Chennai-36, Tamil Nadu,
India

potential risk assessment study revealed that regular exposure to heavy metals through the ingestion pathway caused detrimental health effects. These effects were observed to be more severe in children in comparison to adults.

Keywords PM₁₀ · Elemental characterization · FELXPART · Source apportionment · Health risk

Introduction

The current century has been experiencing an increase in the global economy alongside urbanization and industrialization, which has become widespread across India and many developing (low- and middle-income: LMIC) countries across the globe. In line with such progress are rising levels of atmospheric pollutants across the world. The South Asian region has been reported to be a pollution hub due to the alarming increase in particulate matter (PM) and several gaseous pollutants in the ambient air (South Asia Environment Outlook, 2014). Pertaining to the adverse effect of PM₁₀ (PM with aerodynamic diameter $\leq 10 \mu\text{m}$) on human health and climate systems, it is included as one of the six criteria pollutants in ambient air (World Health Organization-WHO, 2006; US Environmental Protection Agency, 1989). PM₁₀ influences the atmospheric chemistry through its surface reactions, most importantly affecting the tropospheric ozone concentrations and formation of secondary aerosols (Nishanth et al., 2014), while the latter act as a precursor to atmospheric hydroxyl (OH) radicals. In addition, acidic PM₁₀ can cause physical damage to vital installations and infrastructures.

Quantitative estimation of the overall health risks of atmospheric metal particles can lead to early preventive measures and improve health standards. There are many reports on the rise in mortality rate due to PM exposure (Kim et al., 2015; Tao et al., 2014) as a pollutant that may penetrate human respiratory systems causing cardiovascular and pulmonary diseases (Pascal et al., 2014). Heavy metals such as copper (Cu), arsenic (As), nickel (Ni), chromium (Cr), and lead (Pb) present in PM₁₀ also have carcinogenic impacts on inhalation, as discussed by many researchers (Fang et al., 2013; Garcia-Aleix et al., 2014 and references therein). PM₁₀ in ambient air may be

emitted through natural processes like volcanic eruption, crustal sources, sea salt, and gas-to-particle formation, etc., while anthropogenic activities, including vehicular and industrial emissions, agricultural activities, coal and biofuel combustion, waste incineration, soil dust re-suspension, etc. contribute to the overall fraction of emissions, specifically over the urban regions.

The major components of PM₁₀ in the troposphere are mostly in the form of water-soluble inorganic compounds (WSIC), water soluble organic compounds (WSOC), carbonaceous species (elemental carbon (EC) and organic carbon (OC)), and acid-soluble mineral dust (Heintzenberg et al., 1989). The major focus of this study is to characterize the acid-soluble components of PM₁₀ as the lifetime of these particles can range from hours to days in the ambient environment. Further, PM₁₀ particles originating from vehicular non-exhaust often contain various heavy metals, e.g., cadmium (Cd), Pb, Ni, Cu, and zinc (Zn), etc., that are known to have a longer lifetime in the atmosphere (Gugamsetty et al., 2012). The measurement and characterization of PM₁₀, identification of their emission sources, and understanding their influence on human health are indispensable to maintain and regulate the ambient air quality in urban areas. Ongoing research activities on PM₁₀ pollution over Bhubaneswar since the late 1990s have brought out quite some significant scientific information. For example, Mahapatra et al. (2018) reported 3 years of measurements of both PM₁₀ and PM_{2.5} as well as their seasonal variation with meteorological parameters. Das et al. (2011) reported the contribution of water-soluble inorganic component in the atmosphere. The presence of carbonaceous particles (EC and OC) has been discussed in Panda et al. (2016). However, in-depth studies on the physical and chemical characteristics of ambient aerosols, their source, distribution, and influence on human health are crucial to undermine important information that would be pertinent to the scientific community to understand the overall impact of PM pollution. Moreover, the risk assessment of individual elements in ambient aerosols is also quite imperative in terms of air pollution-induced health issues in this region. Hence, this study has the following objectives:

1. Chemical profiling of PM₁₀ with a focus on nineteen different elements such as aluminum (Al), barium (Ba), calcium (Ca), cobalt (Co), chromium

(Cr), copper (Cu), iron (Fe), gallium (Ga), magnesium (Mg), manganese (Mn), nickel (Ni), lead (Pb), strontium (Sr), zinc (Zn), arsenic (As), antimony (Sb), selenium (Se), titanium (Ti), and vanadium (V). These elements are released through various natural and anthropogenic sources into the ambient atmosphere.

2. To conduct microstructural analysis of the collected particles in order to understand and evaluate the particle type, emission sources, and chemical constituents of individual particles through a qualitative analysis of the suspended particles.

3. To use these elements as markers in order to define the sources of PM₁₀ during different seasons using various source apportionment techniques such as PCA, EF analysis, and air mass trajectory analysis (FLEXPART).

4. In addition, to conduct a risk assessment study using United State Environment Protecting Agency (USEPA) standards to understand the influence of heavy metal exposure on human health.

Experimental

Sampling site and general meteorology

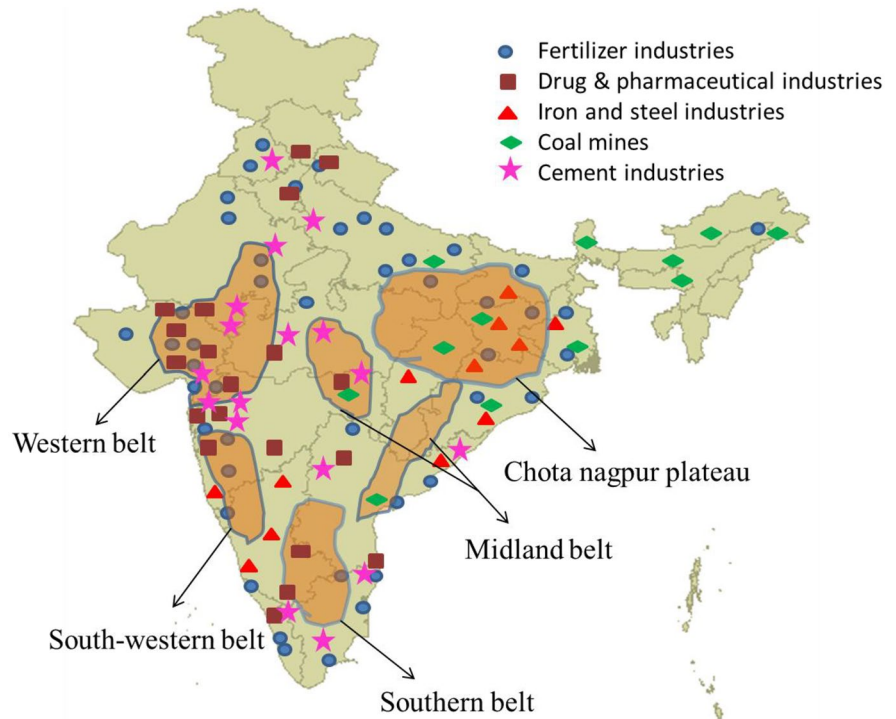
PM₁₀ samples were collected within the premises of the CSIR-Institute of Mineral and Material Technology, Bhubaneswar (21° N, 85° E) by an APM 460 BL, Envirotech make High Volume Sampler (HVS). The

instrument was operated at a constant flow rate of 1.2 m³/min. GF/A Whatman glass microfiber filter paper (8 × 10 in) with a pore size of 1.6 microns was used for the sampling of PM from ambient air. Each filter was weighed before and after sampling by a microbalance (Sartorius CPA225D) with sensitivity ± 0.001 mg (Panda et al., 2015). The instrument was placed at 30 m height on the top of the main building, which is at close proximity to a major national highway (NH-16) in the eastern coast of India. The state capital Bhubaneswar is located in tropical India, ~60 km west of the Bay of Bengal at an altitude of 45 m above mean sea level (Fig. 1). The city has a population of 837,737 and is spread over an area of 419 km² (<http://www.census2011.co.in/census/city/270-bhubaneswar.html>). During the winter season, the city experiences a large outflow of air mass from the most polluted IGP (Indo-Gangetic plain) region. Further, the region is undergoing rapid development due to industrialization, economic growth, and connectivity and is under the influence of several anthropogenic activities including cement industries, thermal power stations, major mines, seaports, fertilizer industries, and metallurgical plants like sponge iron, etc. in the vicinity (Mahapatra et al., 2018) (Fig. 2). Subsequently, the air quality of the city is constantly worsening, specifically in the winter months, and as a result, many pollutants in ambient air were reported to be far above the permissible limit as reported by State Pollution Control Board (SPCB), Odisha.



Fig. 1 India map showing the sampling location Bhubaneswar

Fig. 2 Major industries and mining belt in India



The climate of Bhubaneswar is categorized into four distinct seasons, including pre-monsoon (March to May), monsoon (June to August), post-monsoon (September to November), and winter (December to February) based on the unique weather condition and varying meteorological parameters (Panda et al., 2016). The city receives maximum solar radiation in pre-monsoon months with the highest temperature of 40–45 °C. At the same time, the minimum temperature reaches as low as 10 °C in the winter season. The region experiences heavy rainfall during the monsoon, with a mean value of 220 mm per month.

Sample collection

PM₁₀ sampling was carried out twice a week from July 2012 to August 2013. The duration of each sampling event was approximately 8 h (from 10 am to 6 pm Indian Standard Time) using a HVS at a constant flow rate of 1.2 m³/min (HVS; APM 460 BL, Envirotech; approved by USEPA). The instrumentation and operational mechanisms of the sampler were followed as per USEPA guidelines, and the same methods have been discussed in detail previously (Panda et al., 2016). Weights of the filter papers were taken

in a standardized microbalance (Sartorius CPA225D) with sensitivity ±0.001 mg, before and after sampling.

Quality assurance

Each used filter was conditioned before and after sampling at 25 °C for 24 h in a humidity-controlled desiccator. PM₁₀ mass concentrations were obtained gravimetrically using a microbalance and stored in an airtight zip lock polyethylene container. The filters were weighed three times and the average value of the three measurements was recorded as the actual weight of the paper. The weight differences of the filters before and after collection were considered as the final mass of collected PM₁₀. Samples were not collected in rainy days to ensure instrumental safety.

Two different types of blank filters were considered as control in this study: exposed blank, by keeping a filter paper for 8 h inside the sampler without the supply of air, and filter paper taken straight from the packed filter paper box. Two different blank measurements were performed for every set of 10 samples as per the sampling protocol. Mean blank values were deducted from sample concentrations. The minimum detection limit

(MDL) for each element by ICP-OES has been given in [ST1](#).

Chemical analysis

The sampled and blank filter papers were prepared as reported by Huang et al. (2013) for the elemental analysis using ICP-OES (Wendt & Fassel, 1965). In brief, half of the sampled and blank filter papers were digested at 150 °C for 5 h with 50 ml of a mixed acid solution of concentrated nitric acid (HNO₃), concentrated hydrochloric acid (HCl), and concentrated hydrofluoric acid (HF) (MERCK A.R. grade) at 3:1:1 (v/v) ratio. Then, the digested solutions were allowed to cool at room temperature for filtration using 2.5 µm pore filter papers (Whatman 42) and the volume was made up using Milli-Q water (18 MΩ/cm).

The elements that were measured were Al, Ba, Ca, Cr, Cu, Co, Ni, Fe, Ga, Mg, Mn, Pb, Sr, Zn, As, Sb, Se, Ti, and V. These measurements were done by inductive coupled plasma optical emission spectroscopy (ICP-OES) (Perkin Elmer Optical Emission Spectrometer Optima, Model: 2100DV) first developed by Fassel et al. (1977). The instrument was calibrated using a mixed elemental

standard solution for the quantification of elemental concentrations of samples for every set of five samples.

Morphological analysis

The surface morphology of individual PM₁₀ samples was analyzed using a Carl Zeiss Model: Gemini supra 55 field emission scanning electron microscope (FE-SEM) armed with an energy-dispersive X-ray (EDX) spectrometer. A detailed operating procedure has been discussed elsewhere (Panda & Das, 2017). Transmission electron microscopy (TEM) coupled with an EDX (FEI, Technai G2) was used to capture surface topography of elements present in the collected sample. Sample preparation for both the microscopic analysis has been reported in our previous study (Panda & Das, 2017).

Measurement of meteorological parameters

The temperature, relative humidity (RH), wind speed, and wind direction (Fig. 3) were measured at the sampling location using an AWS (Model: MW8001-01/04; Make: LSI spa).

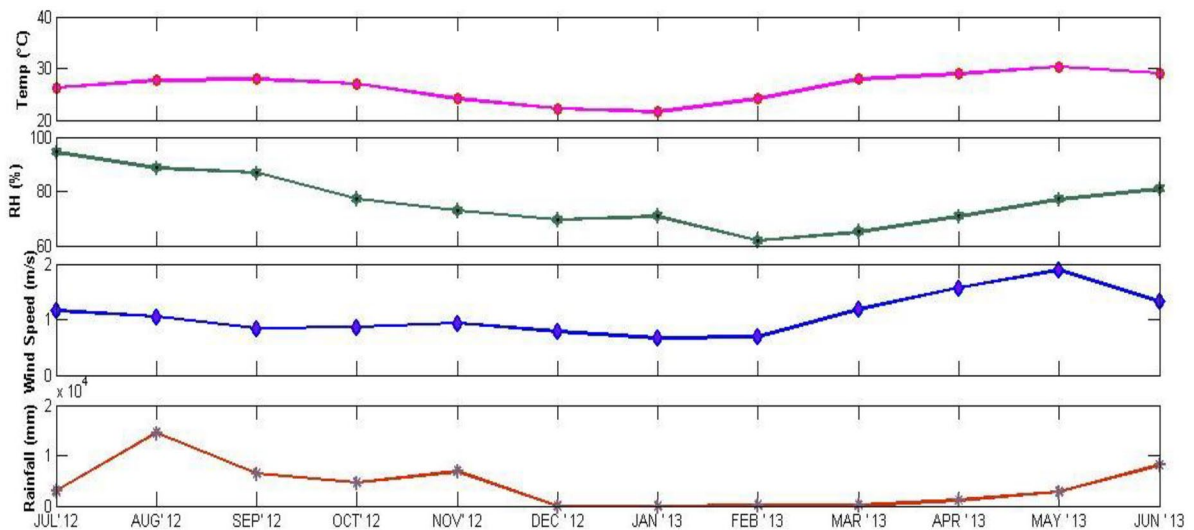


Fig. 3 Seasonal variation of **a** temperature (°C). **b** Relative humidity (%). **c** Wind speed (m/s). **d** Rainfall (mm) during the sampling period

Model description

Impact of incoming air mass from long distance on the elemental composition at the receptor site was evaluated performing 7-day air-mass backward trajectory analysis at 04:30 UTC (Universal Time Coordinated) using the Lagrangian particle dispersion model (LPDM) FLEXPART v10.3 model. The LPDM FLEXPART v10.3 has been used to compute air mass back-trajectory (retroplume) and potential emission sensitivity (PES) fields (Stohl et al., 1998). This has an additional benefit of considering dry and wet deposition in-cloud and below-cloud scavenging over normal trajectory models. Explanation of the FLEXPART model is reported in Seibert and Frank (2004). The input meteorological data from NOAA's National Centers for Environmental Prediction (NCEP) Global Forecast Systems Final (GFS-FNL) data accessible at $1^\circ \times 1^\circ$ horizontal and at 6-h temporal resolution were used here to drive the model. The minimum mixing height was kept at 100 m and the number of particles per run was 50,000. Both output frequency and output integration time were 10,800 s (3 h) for each run along with the other input parameters kept similar to Gadhavi et al. (2015).

Principal component analysis

Theoretically, a principal component can be defined as a linear combination of optimally weighted observed variables. PCA reduces the dimensionality of a data set consisting of many variables correlated with each other, either heavily or lightly, while retaining the variation present in the dataset. This is done by transforming the variables to a new set of variables, which are known as the principal components. PCA was done by using the rotated component matrix to segregate the elemental concentrations into different linear components, each of which was considered as a factor that could provide possible common factors to identify the various sources that contribute to these elements in the ambient PM_{10} .

Result and discussion

Characteristics of ambient PM_{10}

Mass concentration of PM_{10}

Ambient air mass concentration of PM_{10} varied from 5.5 to 276 $\mu\text{g}/\text{m}^3$, with an annual average of

82.28 $\mu\text{g}/\text{m}^3$. Seasonal variation of ambient PM_{10} mass concentration follows a similar trend as previous observations reported in the same sampling site (Mahapatra et al., 2014, 2018; Panda et al., 2015) with maximum mass concentrations observed during winter months (138.24 ± 35 $\mu\text{g}/\text{m}^3$), followed by post-monsoon (69.06 ± 14.138 $\mu\text{g}/\text{m}^3$) and pre-monsoon (66.71 ± 20.41 $\mu\text{g}/\text{m}^3$) seasons. Minimum ambient PM_{10} concentration was observed during the monsoon season (48.43 ± 3.09 $\mu\text{g}/\text{m}^3$). Figure 4 shows seasonal variations of ambient PM_{10} mass concentrations along with their standard deviations. One of the important reasons for the change in seasonal trends is due to the variation in wind patterns. Higher wind speeds during pre-monsoon and monsoon seasons facilitate the dilution of the ambient air pollutants while stagnant atmospheric conditions and lower wind speeds during winter and post-monsoon season enable the build-up in ambient PM_{10} concentrations (Fig. 3). Apart from wind speed and wind direction, rainfall, relative humidity (RH) temperature (Fig. 3), and boundary-layer conditions also have a significant effect on the varying ambient PM_{10} mass concentrations. These observations are in agreement with our previous studies (Mahapatra et al., 2013).

Elemental concentration in PM_{10} and its seasonal variation

As discussed in the previous section, there was a prominent seasonal variation in ambient PM_{10} mass over the site. There was also a distinct seasonal deviation in the percent input of the elements to the overall PM_{10} mass. However, the total average elemental concentrations were more or less similar in all the seasons except for monsoon. Hence, apart from metal particles, a varying contribution of components like carbonaceous particles,

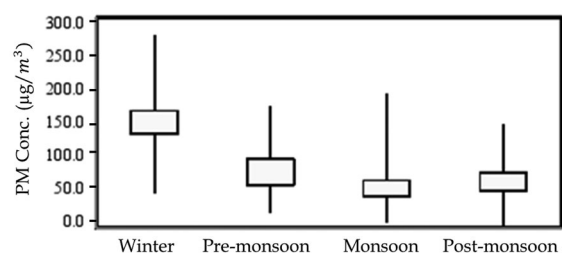


Fig. 4 Seasonal variation in PM_{10} ($\mu\text{g}/\text{m}^3$) concentration during the measurement period

ions, etc. also contribute to the PM₁₀ mass during different seasons. The average elemental concentration was lowest during monsoon ($6.64 \pm 5.6 \mu\text{g}/\text{m}^3$) due to the rain washout effect with a maximum contribution of approximately 13% to the total PM₁₀ mass. However, during the months between March–May (pre-monsoon) and September–November (post-monsoon), the average elemental mass concentration was $7.96 \pm 6.9 \mu\text{g}/\text{m}^3$ and $8.17 \pm 7.19 \mu\text{g}/\text{m}^3$, with a 11.9% and 11.8% contribution, respectively, to the overall ambient PM₁₀ mass (Table 2). However, during winter, the average elemental concentration was $8.32 \pm 8.27 \mu\text{g}/\text{m}^3$ with the lowest percentage contribution of approximately 6% to the overall PM₁₀ mass and was predominantly composed of carbonaceous and other particles from myriad sources. A similar total average elemental concentration was observed during all seasons except for monsoon; therefore, there is speculation about whether they originate from similar sources, which is discussed in later sections.

Elements like Fe, Ba, Al, Zn, Ca, etc., are considered major constituents of coarse mode soil dust particles and were predominant in all the seasons (Li et al., 2004). PM₁₀ mass was also enriched with various heavy metals like As, Cr, Cu, Pb, Co, etc., having a relatively long lifetime in the atmosphere. These

metal concentrations were comparable to other results reported over the Indo Gangetic Plains (Kulshrestha et al., 2009; Sudheer & Rengarajan, 2012). The elemental concentrations of ambient air in Bhubaneswar city are mainly enriched with Al, Fe, Ca, Ba, and Zn (Table 1). However, the individual elemental concentrations were lower than the exposure limits permissible by the Occupational Safety and Health Administration (OSHA), USA, during all the four seasons. This is a positive piece of information for this imminent smart city; however, there is apprehension that exposure to these heavy metals for a prolonged period is likely to induce harmful effects on human health.

Morphology of the metal particles

Analysis of surface morphology of the collected PM₁₀ samples also supports a significant contribution of various metal components to the ambient aerosols of Bhubaneswar along with the dominance of carbonaceous/soot particles (Saffaripour et al., 2020). Basically, three different types of metal-rich particles were observed during the surface study with elemental EDX spectral analysis of individual particles, which also support the PCA analysis results: (1)

Table 1 Elemental composition of PM₁₀ ($\mu\text{g}/\text{m}^3$) during July 2012 to August 2013 at Bhubaneswar represented in four season of the year

	WIN	PRE	MON	POST
Al	1.702 ± 2.3	1.818 ± 1.137	1.061 ± 1.281	1.616 ± 2.327
Ba	2.401 ± 1.531	2.299 ± 1.886	1.509 ± 0.763	2.122 ± 0.469
Ca	1.016 ± 0.612	0.849 ± 0.618	1.009 ± 0.053	1.024 ± 1.341
Co	0.005 ± 0.001	0.006 ± 0.003	0.007 ± 0.003	0.007 ± 0.003
Cr	0.022 ± 0.006	0.020 ± 0.016	0.027 ± 0.014	0.034 ± 0.013
Cu	0.023 ± 0.013	0.019 ± 0.012	0.023 ± 0.019	0.057 ± 0.50
Fe	0.706 ± 1.447	0.286 ± 0.673	0.758 ± 0.092	0.495 ± 0.729
Ga	0.018 ± 0.006	0.012 ± 0.005	0.017 ± 0.013	0.015 ± 0.004
Mg	0.444 ± 0.203	0.597 ± 1.055	0.739 ± 0.561	0.435 ± 0.877
Mn	0.009 ± 0.057	0.034 ± 0.022	0.048 ± 0.071	0.078 ± 0.071
Ni	0.016 ± 0.007	0.027 ± 0.016	0.074 ± 0.134	0.026 ± 0.019
Pb	0.063 ± 0.02	0.033 ± 0.012	0.038 ± 0.023	0.125 ± 0.158
Sr	0.109 ± 0.095	0.147 ± 0.055	0.205 ± 0.070	0.219 ± 0.136
Zn	1.677 ± 1.827	1.745 ± 1.435	1.008 ± 1.962	1.818 ± 0.917
As	0.007 ± 0.003	0.017 ± 0.021	0.016 ± 0.008	0.022 ± 0.015
Sb	0.003 ± 0.001	0.002 ± 0.001	0.002 ± 0.001	0.008 ± 0.007
Se	0.001	0.002 ± 0.001	0.004 ± 0.002	0.005 ± 0.003
Ti	0.0890 ± 0.045	0.046 ± 0.018	0.091 ± 0.121	0.061 ± 0.034
V	0.006 ± 0.002	0.003 ± 0.001	0.005 ± 0.006	0.006 ± 0.004
Total	8.315 ± 8.274	7.961 ± 6.9	6.640 ± 5.686	8.173 ± 7.18

◀**Fig. 5** SEM images and energy dispersive X-ray spectra of **a** A single metal particle with nearly spherical shape dominated by Cr (42.4%), C, and O (>40%) along with traces of Ca, **b** a silicon oxide particle with high intensity of Si and O peak indicating its origin from crustal source, **c** a irregular shaped minerogenic particle characterized by complex mixture of soil-related components like C, O, Al, and Si. **d** The texture of branched cluster of industrial particles with high contribution of Mn, Fe, Co, and Ni by weight

a solitary dense particle with dominant contribution from a single element (Fig. 5a); (2) minerogenic particles with a complex mixture of various soil-related elements like C, Al, and Si etc. with varying percentages (Fig. 5b, c); (3) industrial particles with significant contribution of trace elements like Co, Ni, Mn, Pb, and Cu (Fig. 5d). Detailed analysis of the variation of surface morphology with respect to various seasons of the year has been reported in Panda and Das (2017). The TEM images of the selected particles also reveal that the presence of different elements in atmosphere either mixed with other metals (Fig. 6a) may be referred as a minerogenic particle or in the form of metal oxides such as iron oxide (Fe₂O₃) with branched hexagonal structure (Fig. 6c). The EDAX pattern confirms the presence of a high abundance of Fe peak along with a strong O peak (Fig. 7d). The source of origin of such particles may be from either crustal or industrial emissions.

Source apportionment of PM₁₀

Enrichment factor analysis

Crustal and non-crustal source identifications of various elements detected in ambient PM₁₀ were made using the enrichment factor (EF) analysis. The ratio between different elements from ambient PM₁₀ samples with reference to their typical concentration in the Earth’s crust was taken for respective analysis. Al was taken as a reference element for soil, which is considered to be ideal among the selected elements in the soil (Wedepohl, 1995). The following equation represents a standardized EF for a given element:

$$EF = ([X]/[X_{Ref}])_{Sample} / ([X]/[X_{Ref}])_{Crust} \quad (1)$$

where X is the target element and X_{Ref} is the reference element. Al has been used here as X_{Ref}, as we do not have Si data for this study due to analytical

constraints. The concentration level of all the elements has been derived from Wedepohl (1995). The calculated EF for the selected elements in all four seasons is presented in Table 2. By convention, if the EF is less than 10, it indicates the dominance of crustal sources, while an EF greater than 10 is considered to be enriched by particulate matter from anthropogenic sources (Gugamsetty et al., 2012). During all the seasons, the EF for Zn, Ba, Co, Cr, Sr, Sb, Se, Ni, As, Ga, Cu, and Pb were more than 10, indicating anthropogenic emission sources contributing to these elements in ambient PM₁₀. This could be from the vehicular exhaust and non-exhausts and emissions from various industries in close proximity to the sampling site. Six major thermal power plants and seven of the largest built-in steel plants are located in the north-western sector of the sampling site and contribute significantly to the elemental load (Mallik et al., 2019). Elements such as Mn, Ca, V, Mg, and Ti were found to be less than 10; hence, their predominant origin is from crustal sources. The difference in EF for Fe during different seasons suggests that this element originates from moderate contamination of both crustal as well as anthropogenic segments (Huang et al., 2012).

Source apportionment using PCA

The percentage of total variance and possible sources obtained for the four different seasons of sampling phase are represented in Table 3. There were three principal component factors obtained during the winter season, representing their source of origin. Principal component factor 1 had the highest contributor to the total variance (61.5%) in winter season, which suggests that both anthropogenic and natural emission sources contributed elements such as Al, Ba, Zn, Fe, Ga, Co, Cr, Cu, As, Sb, Ti, Sr, and V. Similar responses were reported by Lough et al. (2005) for the winter season. These elements may have been contributed by local emissions as well as through long-distance transport from crustal/mining and major industrial sources during the sampling period. These elements are mostly present in the form of respective oxides such as Al₂O₃, CaO, TiO₂, Fe₂O₃, SrO, etc. when in the Earth’s crust. The second principal component factor with a total variance of 24.4% is mostly dominated by Mg and Ca with high concentration loading value, clearly suggesting the predominance of aerosols from construction activities in nearby areas. The city is expanding

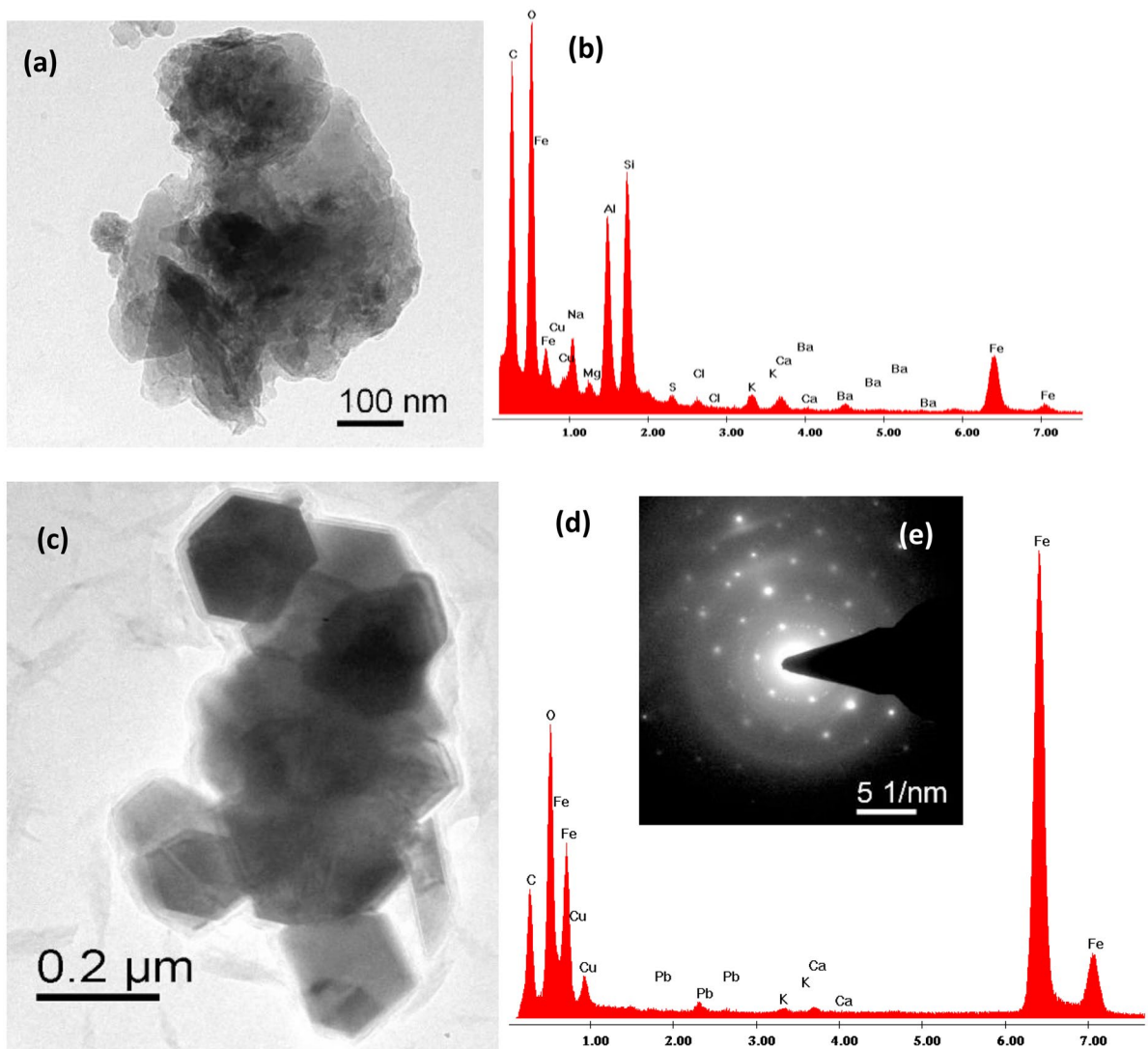


Fig. 6 **a** TEM image. **b** EDX pattern of a mineralogenic particle with traces of Fe, Co, Al, and Si. **c** TEM image. **d** EDX spectra. **e** SAED pattern of Fe_2O_3 particle

quickly and many new skyscrapers and road/bridge constructions were in progress during the sampling period (Economic Survey 2012–13). The third principal component factor with a total variance of 6.8% includes elements like Mn, Pb, and Ni, which are ascribed to be traffic-related non-exhaust sources. The contribution is basically from abrasion processes such as tires, mechanical parts of vehicles, fuel, lubricants, clutch brake pads, regular wear, and tear of other parts of vehicle (Ondracek et al., 2011; Duong & Lee, 2011; Song & Gao, 2011).

During pre-monsoon, the first principal component factor with 80.3% of total variance represents the dominance of Al, Ba, Zn, Fe, Ga, Co, Cr, Cu, As, Sb, Ti, Sr, and V elements indicating mixed emission of sources responsible for the pollution load similar to the winter season. The second principal component factor (total variance of 9.1%) was characterized to be Sb element with a possible source from non-exhaust emissions of motor vehicles (Furusjo et al., 2007). Cu and Ni correspond to the third principal component factor (total variance of 5.2%), which may be treated as markers for nearby industrial emission.

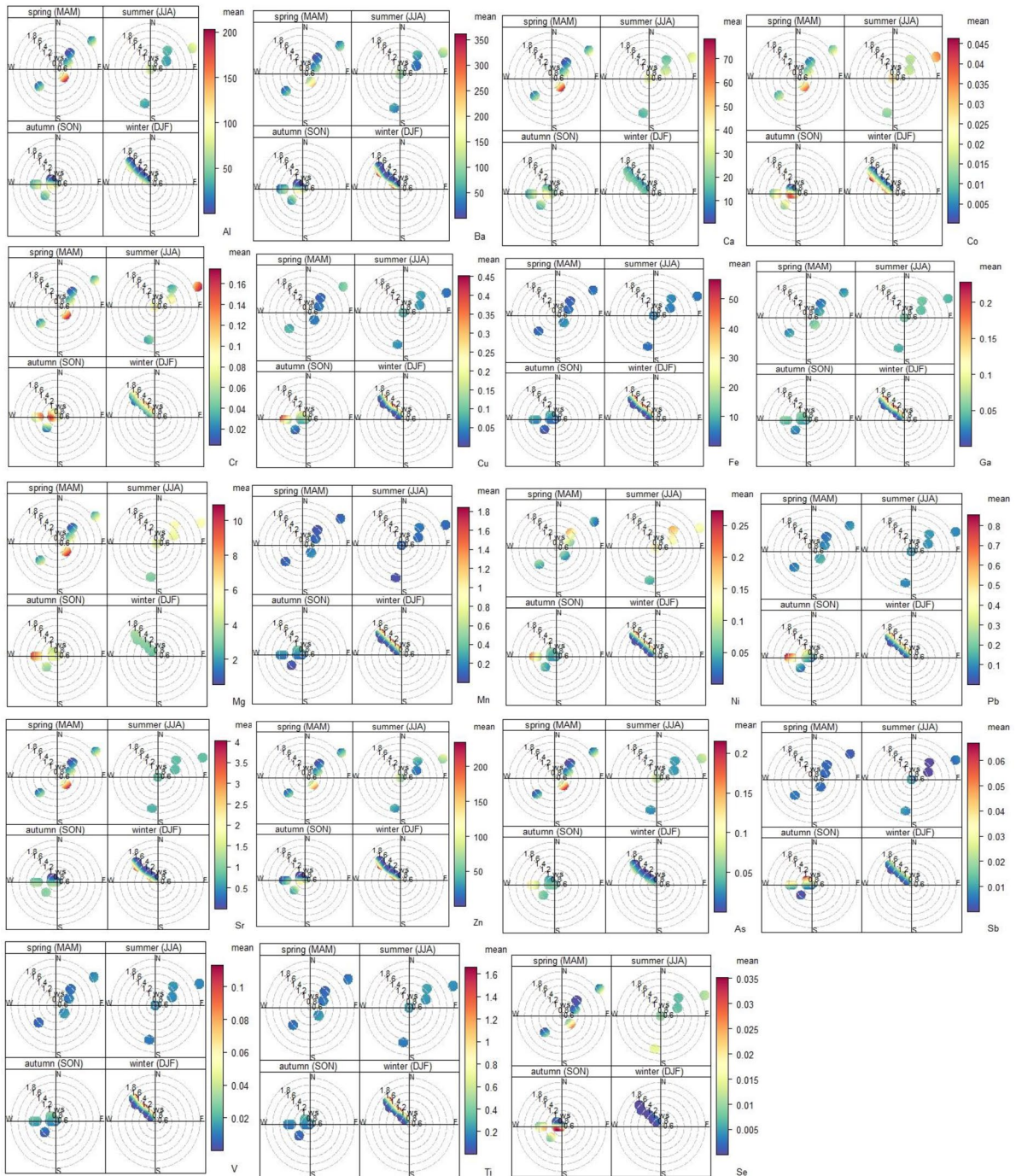


Fig. 7 Polar plot of 19 measured elements (with concentration in color bar) for four different seasons during study period from July 2012 to August 2013 at Bhubaneswar (spring: pre-monsoon, summer: monsoon, autumn: post-monsoon, and winter: winter season)

During the monsoon season, the first principal component factor with 59.7% of total variance represents Fe, Ga, Mn, Cu, Pb, Ni, Sr, Ti, Sb, and V

elements, which could be from industrial activities in the nearby Mancheswar industrial estate located towards the northern part of the sampling site within

Table 2 Enrichment factor for different elements in PM₁₀ during different seasons for the study period from July 2012 to August 2013 at Bhubaneswar

	Winter	Pre-monsoon	Monsoon	Post-monsoon
Ba	163.5	146.6	164.9	152.2
Ca	1.6	1.2	2.5	1.7
Co	17.7	20.4	45.9	30.1
Cr	28.9	24.5	56.5	46.1
Cu	71.8	56.9	115.2	190.8
Fe	10.4	3.9	17.9	7.7
Ga	58.7	35.9	90.5	51.1
Mg	1.5	1.9	4.0	1.5
Mn	1.8	2.8	6.6	7.1
Ni	38.2	61.2	291.6	66.2
Pb	168.2	82.6	162.5	351.4
Sr	15.7	19.8	47.3	33.3
Zn	1467.6	1429.1	1415.6	1675.7
As	159.3	357.9	580.4	522.9
Sb	440.3	219.5	359.8	1180.8
Se	317.2	1104.7	3725.6	3092.9
Ti	1.3	1.6	2.1	1.9
V	5.2	2.8	7.1	5.6

the city (Fig. 1). Principal component factor 2 consists of Al, Ba, Ca, Cr, Mg, Zn, As, and Se with 32% total variance, which could originate from mixed emission sources of crustal or vehicular movements. The crustal source is dominant in all seasons except monsoon due to regular washout effect of re-suspended ambient PM pertaining to rain showers. However, the detection of elements at the observation site is highly influenced by emissions from the small- and large-scale industries placed around the vicinity.

During post-monsoon, three principal component factors were identified; the first factor was dominant (53.8% total variance) with elements such as Fe, Ga, Mn, Sb, V, Ti. This may be due to the possible non-exhaust and vehicular emissions around the sampling site, provided its vicinity close to the NH15, which is one of the busiest highways in the country (Economic Survey 2012–13). Principal component factor 2 signifies Cu, Mg, Ni, Pb, Sr, and As, elements that are usually considered to be the tracers for industrial emissions. Elements such as Al, Ba, Ca, Cr, Zn, and Se were representative of principal component factor 3, which are believed to be of crustal origin and some contribution from industrial emissions as well.

During all the seasons, various element components in PM₁₀ mass originated from mixed sources. Mostly vehicular non-exhaust, construction activities, traffic-based emissions, crustal and industrial sources were the key components contributing to the various elemental components detected in the PM₁₀ mass.

Concomitant source identification of Zn and Ba

The average elemental concentration of PM₁₀ samples over Bhubaneswar was compared with elemental data reported from other sites across the globe (Table 4). Most of the elemental concentrations detected in Bhubaneswar were nearly similar to the other cited locations; however, the relatively higher concentrations of Zn and Ba in comparison to other urban locations, including polluted cities such as Delhi, Kolkata, and Agra, were reason for further speculation. In addition, EF values were consistently greater than 100 for both of these elements during all the four seasons, which indicates that their origin was from non-crustal sources (Table 2). Additionally, wind data (Fig. 7; details in “[Role of local meteorology](#)” and “[Impact of long-range transport of the air mass](#)”) indicates that the source of these two elements is predominantly from the nearby industrial area located within 5 km on the north-northeast direction of the sampling location (Fig. 1). The same is corroborated by the data provided by District Industries Centre (DIC) Bhubaneswar. The information showed that there are more than 30 galvanizing, casting, mineral, and metal-based industries, along with four pharmaceuticals in the industrial estate area. In particular, Mancheswar has a great potential to emit Zn from these industries, as well as Ba from various lubricants used in machines. All these industries are actively functional during the daytime to meet the public demand resulting in the emission of the high amount of metal particles to the ambient atmosphere.

Ba enters into the atmosphere mostly through mining activities, refining processes, and during the production of barium-related compounds. Further, a major part of Ba emission may occur from vehicles due to the addition of Ba compounds in fuel for the reduction of black smoke emission from diesel engines (Turley et al., 2012); however, there is no quantitative information presently available in this regard. Soluble Ba compounds are known to cause ‘Baritosis’ upon inhalation along with various other

Table 3 Principal component analysis (PCA) of multi-elements during different seasons

	Factor 1	Factor 2	Factor 3
Winter Variance in % Sources	Al, Ba, Zn, Fe, Ga, Co, Cr, Cu, As, Sb, Ti, Sr, V 61.5 Mixed source (anthropogenic/natural)	Ca and Mg 24.4 Crustal/construction	Mn, Ni, Pb 6.8 Vehicular non-exhaust
Pre-monsoon Variance in % Sources	Al, Ba, Zn, Fe, Ga, Co, Cr, Cu, As, Ti, Sr, V 80.3 Mixed	Sb 9.1 Non-Exhaust	Cu, Ni 5.2 Industry
Monsoon Variance in % Sources	Fe, Ga, Cu, Mn, Ni, Pb, Sr, Sb, Ti, V 59.7 Industrial	Al, Ba, Ca, Cr, Mg, Zn, As, Se 32.9 Mixed	
Post-monsoon Variance in % Sources	Fe, Ga, Mn, Sb, V, Ti 53.8 Non-exhaust and vehicular emissions	Cu, Mg, Ni, Pb, Sr, As 30.46 Tracers for industrial emissions	Al, Ba, Ca, Cr, Zn, Se 12.23 Crustal

health issues (Sax, 1968). In spite of the higher concentration of Ba, people of Bhubaneswar are still relatively safe as the 8-h annual average of Ba is 2.1 µg/m³ over the site (8-h threshold limit in ambient air being 500 µg/m³ as per American Conference of Governmental Industrial Hygienists).

In addition, another important source for measured heavy metals, including Zn and Ba, could be from various electronic wastes (e-waste). E-waste includes television, mobiles, laptops, desktops, servers, electronic toys, and cooling units such as refrigerators and air conditioners, which are difficult to recycle in a sustainable manner. India is the producer of more than 3.5 lakh tons of e-waste per annum, of which only 23 units are registered with Government of India for the entire recycling processes (Monika, 2010). The remaining e-waste is discarded in an unorganized way, mostly by “rag pickers” who collect e-waste from residential areas and destroy it to get sellable by-products. The remaining e-waste is generally dumped in municipal landfill sites, which can co-emit various toxic heavy metals due to some illegal burning of the municipal landfill site (Gullett et al., 2007). The probability of heavy metal emissions during e-waste segregation is also quite high. For instance, a cathode ray tube (CRT) is made of nano-sized Ba and Zn metal particles packed inside the tube, and when it is either broken or incinerated during the segregation process, the metals are released into the ambient air. The sample site is 2 km away from the shantytown where such unorganized segregation activity occurs. Furthermore, Zn is one of the components required in the manufacturing of steel alloys, disposable and rechargeable batteries, luminous materials, etc., while Ba is one of the additives for manufacturing electronic phototubes and is also used as a filler in plastic and rubber goods, as well as lubricant manufacturing and other industries (Sivaramanan, 2013). These could be probable emission sources for Zn and Ba detected over the site.

Role of local meteorology

A myriad emission sources, such as vehicular exhaust and non-exhaust, crustal, and industrial sources, make major contributions to various elements detected in PM₁₀ mass for all four seasons. To further understand the effect of meteorological parameters, especially local wind patterns, on having a significant influence in the PM₁₀ composition, a polar plot was generated (Fig. 7) over the location for the sampling period.

The observation establishes a link between wind patterns and specific emission sources of each element detected in the PM_{10} sample.

During winter (DJF), wind flows only from the north-west direction, while the average elemental concentration was also highest during this season. Our earlier reports (Mahapatra et al., 2018; Mallik et al., 2019) have supported the observation that various aerosols and gaseous pollutants are contributed by the transport of air masses, especially from the north-western sector, which harbors the major industrial and mining belt of Odisha state (Fig. 2). Hence, it could be inferred that during winter months of this sampling period, wind masses carried the elements to the site from these sectors. However, during pre-monsoon and monsoon seasons, the wind pattern was oriented along with the northeastern sector, indicative of the incoming polluted air from the nearby Mancheswar industrial estate and from vehicular emissions from the busy National Highway 16, which is also towards the northeastern part of the sampling site. This strongly supports the major contribution of local emission sources to various metal components in PM_{10} mass. In the post-monsoon season, the wind pattern was mostly centralized, which further justifies the impact of local emission sources on the elemental concentration.

Impact of long-range transport of the air mass

The three-dimensional PES maps are represented in Figs. 8, 9, 10, and 11, and their corresponding values are given at the right side of each row in the logarithmic color scale. It has been observed that the incoming air pattern was distinct during different seasons of the year, and the elemental concentration was strongly influenced by several factors like wind speed, the path traveled by the air mass, i.e., on land/ocean, the origin of air trajectories, etc. Furthermore, in all of the sampling days, the highest PES values were observed near the sampling site, indicating the influence of regional emissions on the air quality of Bhubaneswar.

Winter During winter months, elemental concentrations were determined for six different days (2 days in each month) and the air parcels travelled mostly from the northwestern part of the country (Fig. 8) in most of the sampling days. However, on 17th Dec 2012, the PES region shifted towards the north-central part where the major mining belt of India, such as Chhota Nagpur plateau and midland

mining belt, are situated resulting in higher elemental concentrations on that day as the plume picked more elements from these areas (Fig. 2). On 27th Dec 2012 and 22nd Jan 2013, the retro plumes were coming from the north-western part of the country without much change in sensitivity, resulting in nearly similar total concentration of the measured elements. On 8th Jan 2013, even though the air had traveled from the polluted IGP region, the air samples exhibited the highest PES value and the lowest elemental concentrations of the season. However, this can be explained by the air spending quite some time over the marine environment of the Bay of Bengal (BoB) before reaching the sampling. On the contrary, the PES was lowest and elemental concentrations were highest on 11th and 18th Feb 2013, where major iron and steel industries, namely Tata Steel, Kalinganagar, Nilanchal Ispat Ltd., etc. and the mining belt, are located. Furthermore, on 11th Feb 2013 when the elemental concentration was noted to be highest, this observation might be due to the incoming air mass carrying additional pollutants from the midland mining belt (Fig. 2) with a relatively narrowed PES region, which facilitates the concentration of pollutants. Whereas on 18th Feb 2013, the PES region also covers some parts of the marine environment, resulting in dilution of the pollutants.

Pre-monsoon In pre-monsoon (Fig. 9), the analysis was done for five different sampling days (one from March and 2 samples each from April and May). It was observed that, during 9th April, 24th April, and 16th May 2013, even though the site had received incoming air from both the south and north-western part of India, the high PES extended along the southern coastal part of the landmass over the Vizag steel plant and the Vishakhapatnam port, where dockyard and ship building are frequent activities. Furthermore, the wind plume blew over Ganjam district of Odisha state before reaching the observation site with a significant PES value (Table 3). This district is home to several exploitable mineral deposits like rutile, lamenite garnet, sillimanite, zircon etc., as well as a myriad of manufacturing factories like chemical, allied, agro-based, glass and ceramics, engineering, metal-based, electrical, granite cluster, service, and repair etc. Therefore, there might be a substantial contribution of various metals to the air mass passing through this sector, causing the highest concentration

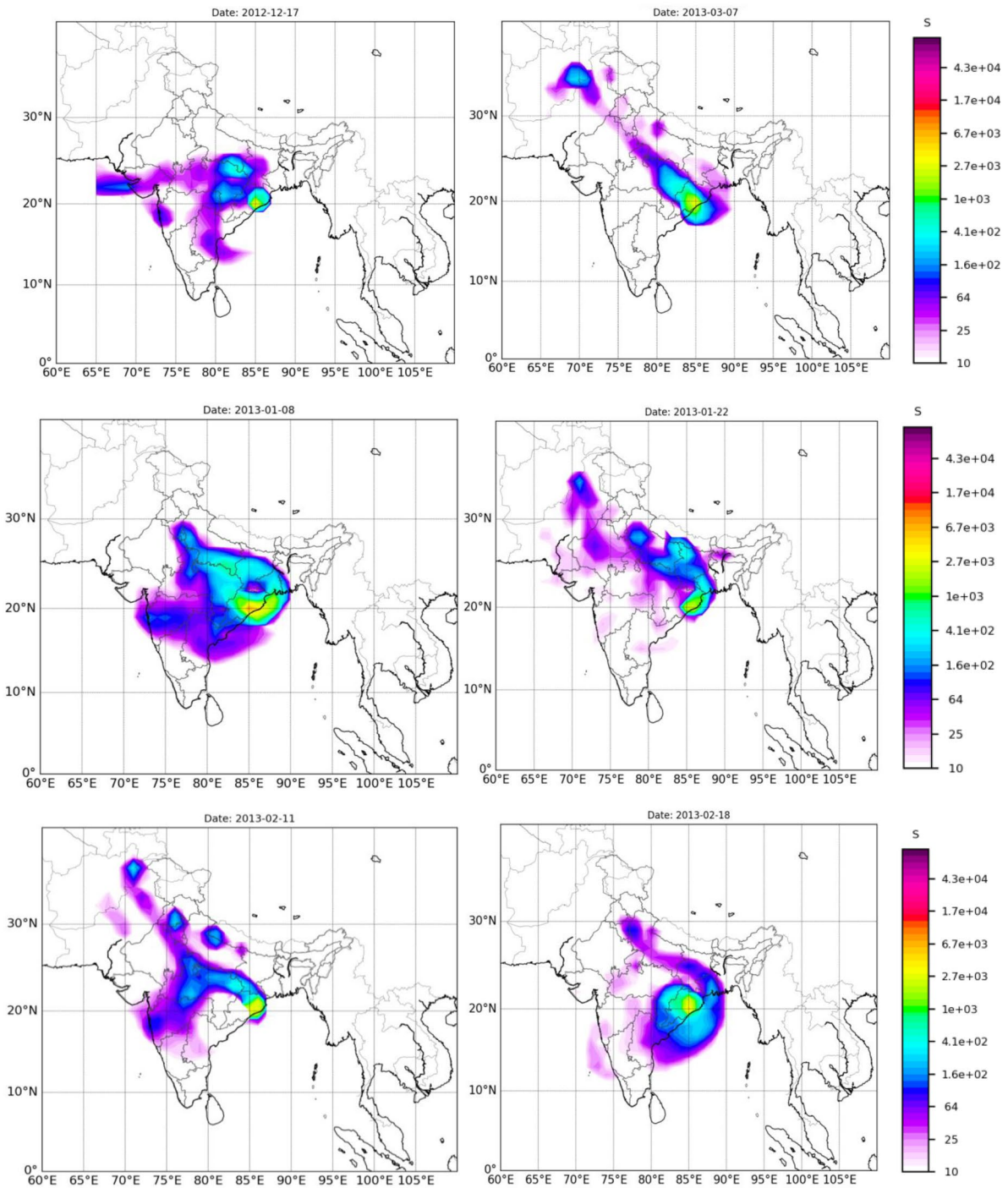


Fig. 8 Potential emission sensitivity (PES) maps for Bhubaneswar during the sampling days in winter months using 7 days of retro plumes of FLEXPART where ‘s’ is the sensitivity in second

of the season on 9th April. However, on 16th May 2013, the average elemental concentration was comparatively lower, which was attributed to higher

temperatures (daily average 30.1 °C, highest in comparison to all the other observation days in this season) leading to dilution even though the wind plume

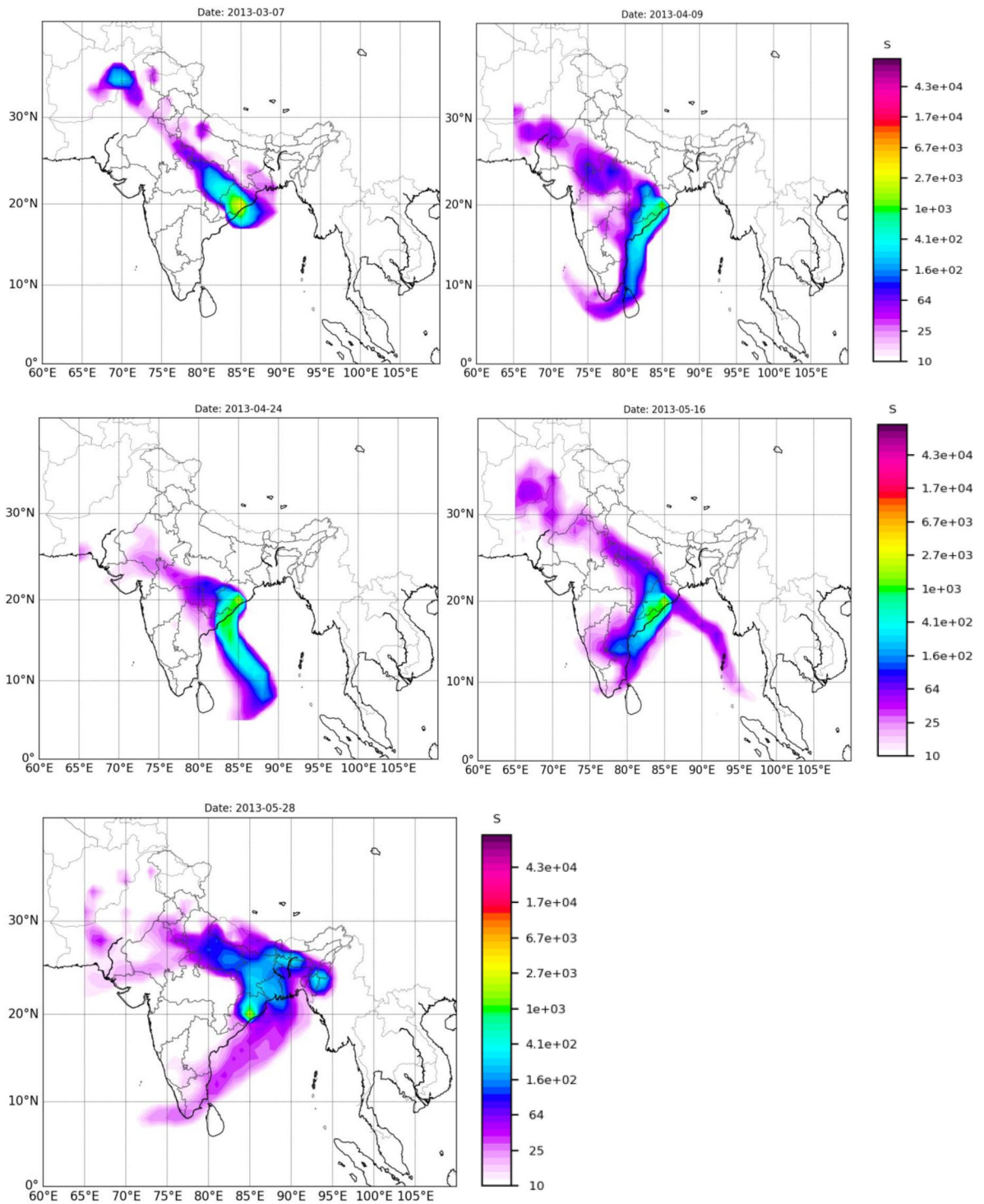


Fig. 9 PES maps during the sampling days in pre-monsoon seasons using 7 days of retro plumes of FLEXPART

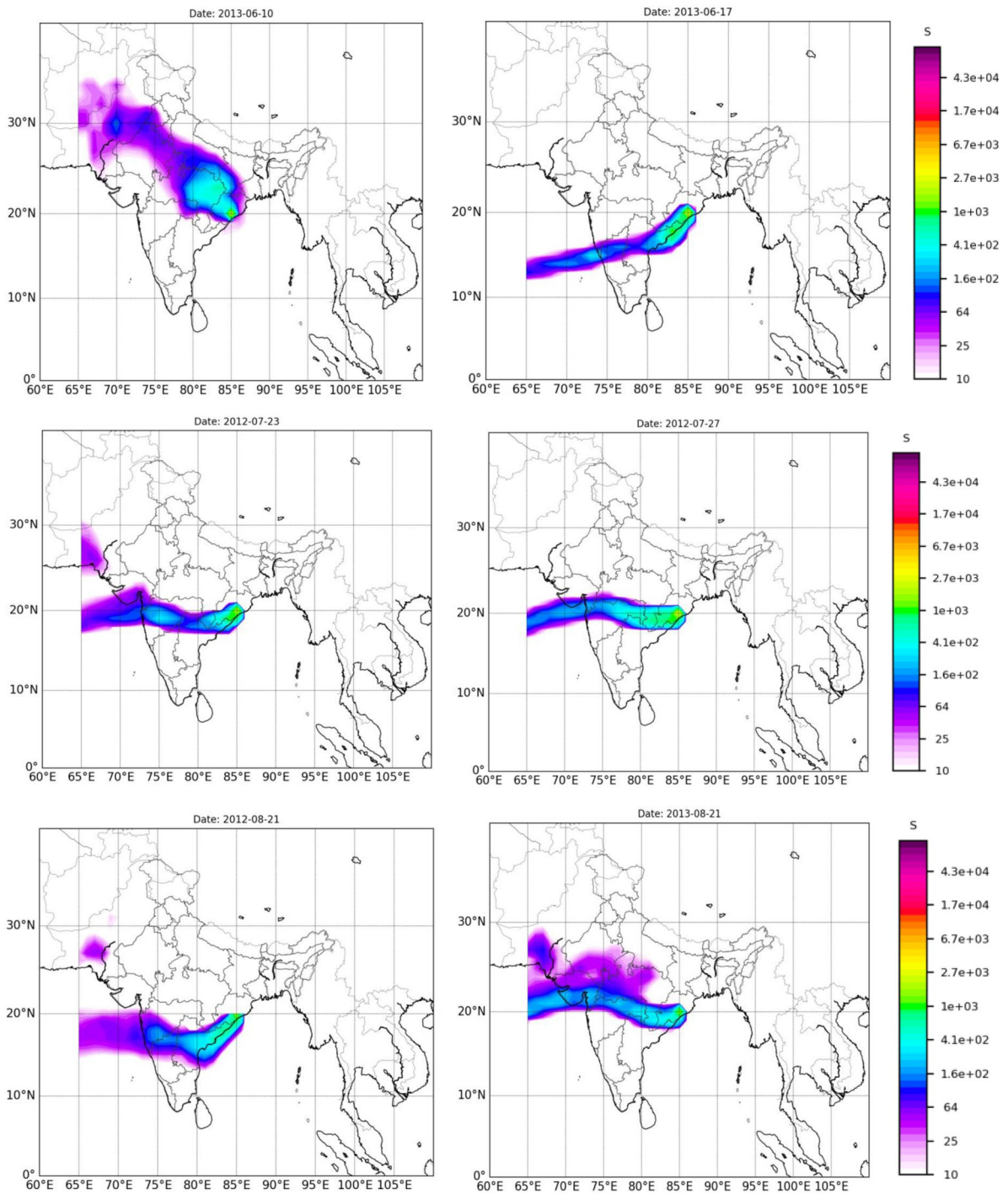
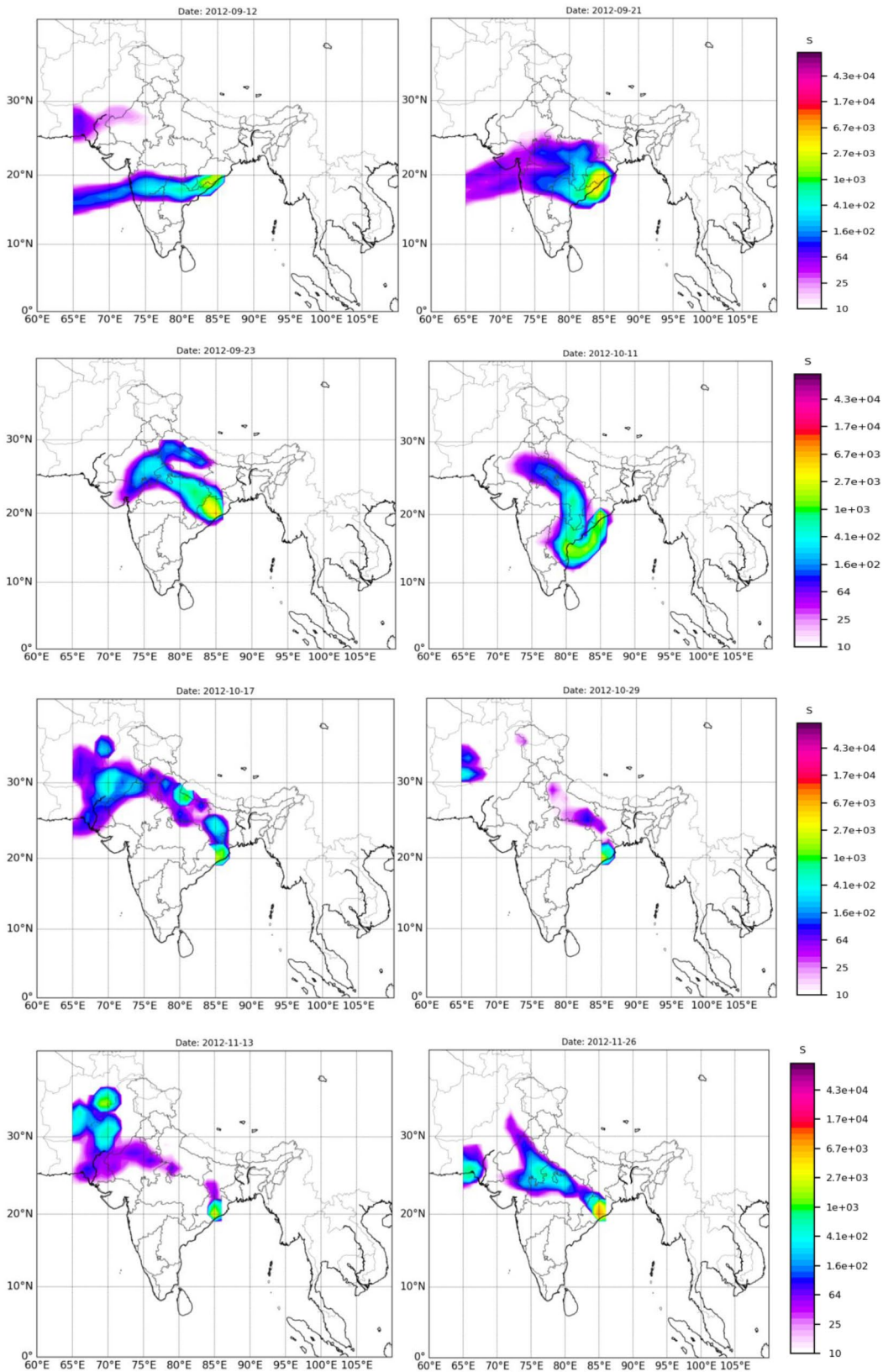


Fig. 10 PES maps during the sampling days in monsoon season using 7 days of retro plumes of FLEXPART

has traveled through southern landmass area. Further, on the 7th March and 28th May 2013, the PES region shifted to the north-western part of the sampling

site. Particularly on 7th March 2013, a little part of the PES region covered BoB and moved further over the Khordha and Puri coasts of Odisha state, then



◀**Fig. 11** PES maps during the sampling days in post-monsoon season using 7 days of retro plumes of FLEXPART

narrowed up towards central India. Puri, being a popular travel destination, also attracts thousands of tourists round the year; therefore, there is a high chance of contribution of emissions from vehicles and other anthropogenic activities. On 28th May 2013, the PES region wind plume traversed again towards the north-western sector, which is home to several industries such as Odisha Sponge Iron Ltd., Tata Steel, and Bhusan Steel Ltd. In addition, this sector also harbors large chromite open-pit mines.

Monsoon During the monsoon months (Fig. 10), analysis was carried out only for six different sampling days (two from each month). The wind plume traveled systematically from the western part of the country over Maharashtra, Andhra Pradesh, Chhattisgarh, and sometimes Gujarat during all the sampling days except 10th June 2013. However, 27th July 2012 had the lowest average elemental concentration, which may be attributed to 70 mm of rainfall recorded over the site on that particular day. All the other sampling days were considered dry days with no rain event. On the 21st August 2012, the wind plume hit the landmass near the Andhra Pradesh coast and then moved towards the observation site, traversing the polluted and industrialized Vishakhapatnam city and southern coastal part of Odisha state, which contributed to the overall elemental mass. However, the highest average elemental concentration was observed on 17th June 2013, although some parts of the PES region covered the marine environment of the BoB. Only Zn, Ba, Ca, and Al contributed to more than 90% to the overall elemental concentration. On 10th June 2013, the PES pattern moved entirely to the continental sector of the north-central part of the country, picking up the pollutants from Chhotanagpur plateau, resulting in a higher average elemental concentration in comparison to most sampling days during this season.

Post-monsoon During post-monsoon (Fig. 11), the elemental analysis was done for eight different days (two from November and three from each September and October). Though the wind plume mostly traveled either from the north-western or south-central

parts of the country, the PES pattern for all of them were very much distinct from each other. On 12th Sept 2012, the PES region mainly covered the western and central parts of India through parts of Maharashtra, Telangana, and Andhra Pradesh, before reaching the observation site through the southern part of Odisha state. These sectors have many urban areas along with mining belts that contribute to the metals in the PM_{10} mass. On 21st September 2012, though the PES region covered the south-central landmass of the country, it became more significant when it entered the marine coast before moving towards the observation site. On 11th October 2012, the wind plume originated from central India and traversed down to the southeastern coastal belt before entering the Bay of Bengal for a few hours, then hitting the landmass and traveling towards the observation site. The wind speed was lowest on this particular day, which could have facilitated the trapping of the local emissions as discussed earlier. On 17th October, 29th October, and 13th November 2012, the wind plume traveled from the extreme north-western sector of the country through the polluted IGP region, where various anthropogenic components that contribute to the PM_{10} mass and the metals as well (Devi et al., 2020). Further, along the journey, the PES was more significant on 17th Oct over the northeastern part of Odisha state, harboring major mining belts, which might have added to the elemental concentration of the already polluted air mass. Therefore, the maximum average elemental concentration was observed on this date. However, on 26th Nov 2012, the sum of the total elements was observed at its lowest concentrations. A possible explanation for this could be that the travel pathway of air mass on this particular day traversed through a cleaner area in between the IGP and midland mining belt of India (Fig. 2). Hence, most likely would carry clean air mass with lesser metal particles.

Health risk assessment

Carcinogenic excess cancer risk of metals in PM_{10}

The PM_{10} -bound total concentrations of the metals are calculated for the possibility of excess cancer risks (ECRs) with a unit risk. Two basic assumptions have been considered for this calculation; firstly, all the heavy metals got into the body through the lungs;

Table 4 Average metal concentration of PM₁₀ (µg/m³) samples collected at Bhubaneswar and comparison with reported data from other locations in India as well as across the world

Sampling location	Al	Zn	Mn	Fe	Mg	Ca	Ba	Cr	Cu	Ni	Co	Pb	As	V	Ti	Sr	PM ₁₀	Year
Visakhapatnam ^a	4.09	0.677	0.154	2.74	-	-	-	0.007	0.003	0.006	-	0.009	0.003	0.004	-	-	65.4	2010–2011
Brahmaputra Valley ^b	4.32	-	0.03	1.42	-	-	-	0.06	0.02	0.05	0.002	0.06	-	-	-	-	52.5	-
Delhi ^c	2.5	0.58	0.08	2.5	-	-	0.32	0.039	0.074	0.012	-	0.43	0.048	0.019	0.33	0.046	-	2008
Delhi ^d	3.26	0.76	0.12	0.61	1.02	7.51	-	0.17	0.07	-	-	0.07	0.13	-	0.16	-	249.71	2013–2014
Ahmedabad ^e	5.92	0.159	0.119	0.398	-	-	0.067	0.011	0.028	0.01	-	0.228	-	-	-	0.039	-	2006–2007
West Bengal ^f	-	0.23	0.06	-	-	-	-	-	0.06	0.031	-	-	-	-	-	-	308.84	2014–2015
Agra ^g	-	0.5	0.9	2.9	-	-	-	0.3	0.1	0.2	-	1.1	-	-	-	-	154	2006–2008
Bhubaneswar ^h	6.197	6.249	0.009	1.676	1.325	3.898	8.331	0.022	0.023	0.016	0.005	0.063	0.015	0.005	0.072	0.17	80.612	2012–2013
Makkah, Saudi Arabia ⁱ	0.29	-	-	-	-	-	-	0.02	-	-	-	0.07	0.28	0.01	-	-	233.38	2015
Chiang Mae, Thailand ^j	0.31	-	-	-	-	-	-	-	-	0.1	-	0.05	0.2	0.01	-	-	73.6	2012
Nam Co, Chaima ^k	0.352	0.002	0.005	0.207	0.106	0.277	0.003	0.004	-	0.001	-	0.001	-	0.001	-	0.002	-	2005–2007
Lampedusa, Italy ^l	0.36	-	0.005	0.304	0.004	0.862	-	-	0.002	0.002	-	-	-	0.005	0.003	0.007	32	2007–2008

^aPolice et al. (2016)
^bBhuyan et al. (2018)
^cPerrino et al. (2011)
^dSharma et al. (2015)
^eSudheer and Rengarajan (2012)
^fGhosh et al. (2018)
^gKulshrestha et al. (2009)
^hPresent study
ⁱChantara (2012)
^jHabeebullah (2016)
^kKang et al. (2016)
^lCalzolari et al. (2015)

secondly, the metal concentrations found from PM₁₀ signify the absolute ambient concentrations of the measured metals. Statistical data about carcinogenicity and unit risks for the metals used in this study were acquired from USEPA IRIS (Integrated Risk Information System) (USEPA, 1998) (<http://www.epa.gov/iris/>). ECR is calculated with the following empirical equation (Hieu & Lee, 2010; Park et al., 2008):

$$ECR \text{ (inhalation)} = \text{Conc. of pollutants } (\mu\text{g}/\text{m}^3) \times \text{unit risk } (\mu\text{g}/\text{m}^3)^{-1}.$$

One-seventh of the total Cr concentration is considered to be Cr(VI) and is used in the calculation of carcinogenic risk, since the proportion of carcinogenic Cr(VI) to non-carcinogenic Cr(III) in the atmosphere is around 1:6. Of all the measured elements, Cr, Ni, Pb, and As are known carcinogens that cause serious health risks by inhalation path (Hieu & Lee, 2010). The USEPA has categorized the atmospheric pollutants into five different groups including.

1. Human carcinogen (group A).
2. Probable human carcinogen (B1 and B2).
3. Possible human carcinogen (C).
4. Not classifiable as to human carcinogenicity (D) and.
5. Evidence of non-carcinogenicity for humans (E).

Cr (VI), Ni, and As are considered to be important human carcinogens through the inhalation route of exposure and are categorized as group A. Similarly, Pb is grouped as a probable human carcinogen (group B2). According to the literature, the observed concentrations fall within a range of 10⁻⁶ to 10⁻⁴ which does not indicate any risk for carcinogenicity (Hu et al., 2012). The ECR value of the five analyzed metals, namely Cr (VI), Ni, Pb, and As, in PM₁₀ are in the order of post-monsoon > monsoon > pre-monsoon > winter (Table 5). The Cr (VI) and As were found to be dominant during all seasons, with annual average ECR values of 4.4 × 10⁻⁵ and 6.7 × 10⁻⁵, respectively. However, Pb had the lowest risk of carcinogenicity through the inhalation route with an observed ECR of 7.8 × 10⁻⁷, followed by Ni, which had an ECR of 8.6 × 10⁻⁶ annually. The total annual average ECR values for the four different heavy metals in Bhubaneswar were found to be 1.2 × 10⁻⁴,

Table 5 Excess cancer risk of carcinogenic elements in PM₁₀

Element	Carcinogenic group	C, Concentration in μg/m ³				Inhalation unit risk (μg/m ³) ⁻¹	Excess cancer risk (μg/m ³) ⁻¹			
		Pre-monsoon		Monsoon			Post-monsoon		Winter	
		Winter	Pre-monsoon	Monsoon	Post-monsoon		Winter	Pre-monsoon	Monsoon	Post-monsoon
Cr (VI) ^a	Group A (human)	0.022	0.02	0.027	0.034	1.2 × 10 ⁻²	3.77E-5	3.43E-5	4.6E-5	5.83E-5
Ni	Group A (human)	0.016	0.027	0.074	0.026	2.4 × 10 ⁻⁴	3.84E-6	6.48E-6	1.76E-5	6.24E-6
Pb	Group B2 (probable human)	0.063	0.033	0.038	0.125	1.2 × 10 ⁻⁵	7.56E-7	3.96E-7	4.56E-7	1.56E-6
As	Group A (human)	0.007	0.017	0.016	0.022	4.3 × 10 ⁻³	3.01E-5	7.31E-5	6.86E-5	9.46E-5
	Total					Total	7.24E-5	1.11E-4	1.33E-4	1.61E-4

^aCr(VI) concentration is 1:7 of total Cr concentration

which is in the range of the permissible limit of exposure.

Potential risk assessment for human health

The purpose of potential risk assessment is an estimation of the intensity, frequency, and duration of human exposure to the pollutant. In this study, the average daily intake (ADI) through three different modes of exposure (ingestion, inhalation, and dermal contact) to heavy metals has been identified separately for adults and children because of their behavioral and physiological differences (Hu et al., 2012; Kong et al., 2012; Singh & Kumar, 2017).

Average daily intake through ingestion pathway (ADI_{ing}, mg/kg/day)

$$ADI_{ing} = (C \times IngR \times EF \times ED \times CF) / (BW \times AT)$$

Average daily intake through inhalation pathway (ADI_{inh}, mg/kg/day)

$$ADI_{inh} = (C \times InhR \times EF \times ED) / (BW \times AT \times PEF)$$

Average daily intake through dermal contact (ADI_{derm}, mg/kg/day)

$$ADI_{derm} = (C \times SA \times AF \times EV \times ABS \times EF \times ED \times CF) / (BW \times AT)$$

In the above equation,

C is the elemental concentration in PM₁₀ (mg/kg)

IngR—ingestion rate (mg/day)

InhR—rate of inhalation (mg/day)

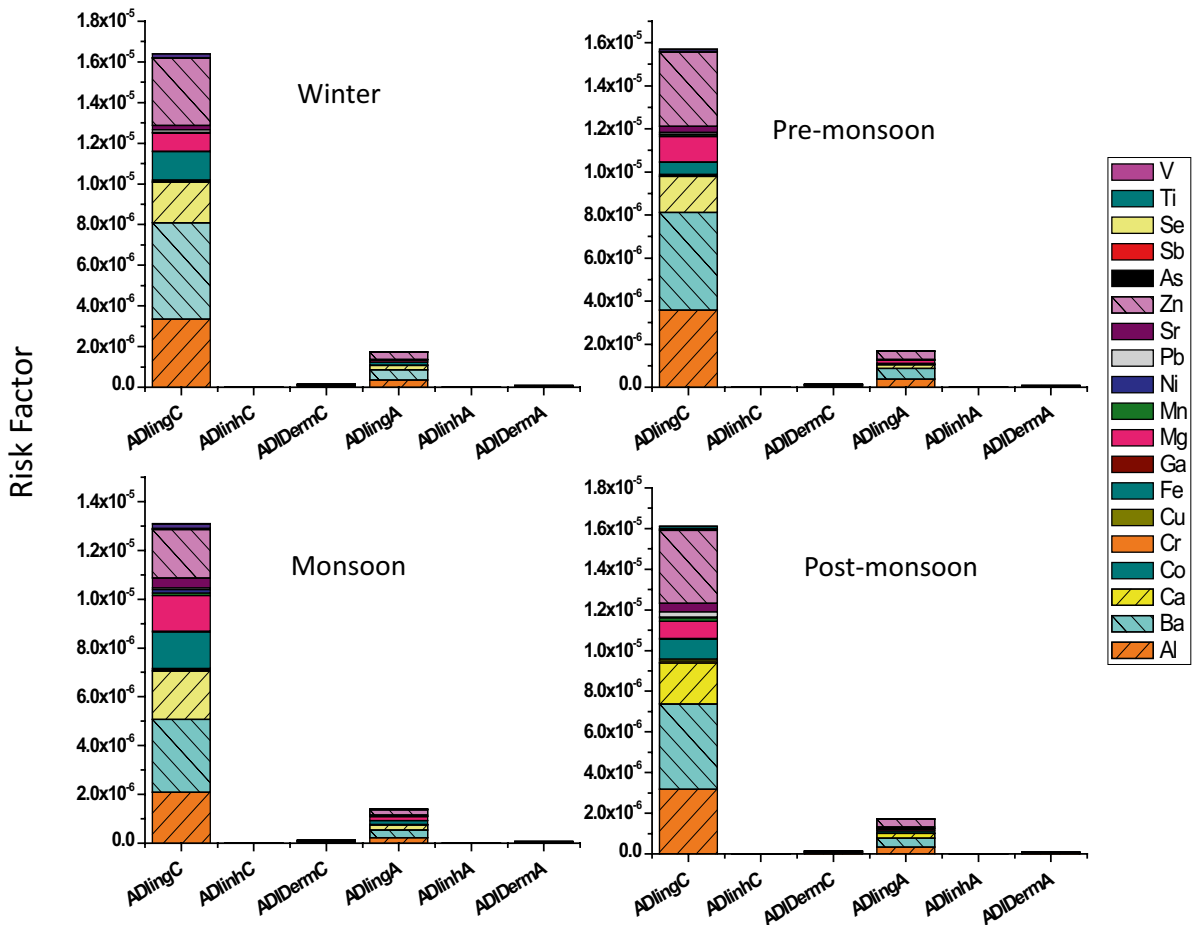


Fig. 12 Potential health risk assessment results via all the three exposure pathways for measured metals during different seasons (C: children and A: adult)

Table 6 Recommended values of reference doses (RfD) (mg/kg/day)

Heavy metals	Co	Cr	Cu	Ni	Pb	Zn	V
RfD _{ing}	3×10^{-4}	3×10^{-3}	4×10^{-2}	2×10^{-2}	3.5×10^{-3}	3×10^{-1}	7×10^{-3}
RfD _{inh}	5.71×10^{-5}	2.86×10^{-5}	4.02×10^{-2}	3.52×10^{-3}	3.52×10^{-3}	3.01×10^{-1}	7×10^{-3}
RfD _{derm}	NA	6×10^{-5}	1.2×10^{-2}	5.4×10^{-3}	5.25×10^{-4}	6×10^{-2}	7×10^{-5}

RfD_{ing} RfD for ingestion, RfD_{inh} RfD for inhalation, RfD_{derm} RfD for dermal contact

EF—exposure frequency (180 days/year)
 ED—exposure duration
 BW—body weight
 SA—skin surface area
 AF—adherence factor of soil to skin
 EV—events frequency
 ABS—the dermal absorption fraction
 PEF—particle emission factor in m³/kg
 AT—averaging time for non-carcinogens = ED × 365 days/year
 CF—conversion factor
 All the factors used for the above calculations have been adopted from the US EPA due to the lack of

local exposure parameters for health risk assessments (US EPA, 2007; US EPA, 2009).

Potential health risk assessment results via all the three exposure pathways for measured elements during different seasons are summarized in Fig. 12. It is observed that the risk factor was maximum when exposed through ingestion pathway. The average daily metal exposure for adults is ten times lower than children for all the studied pathways, which indicates that children are more vulnerable to exposure to pollutants than adults; therefore, the determination of toxic organic compounds, i.e., VOC (volatile organic

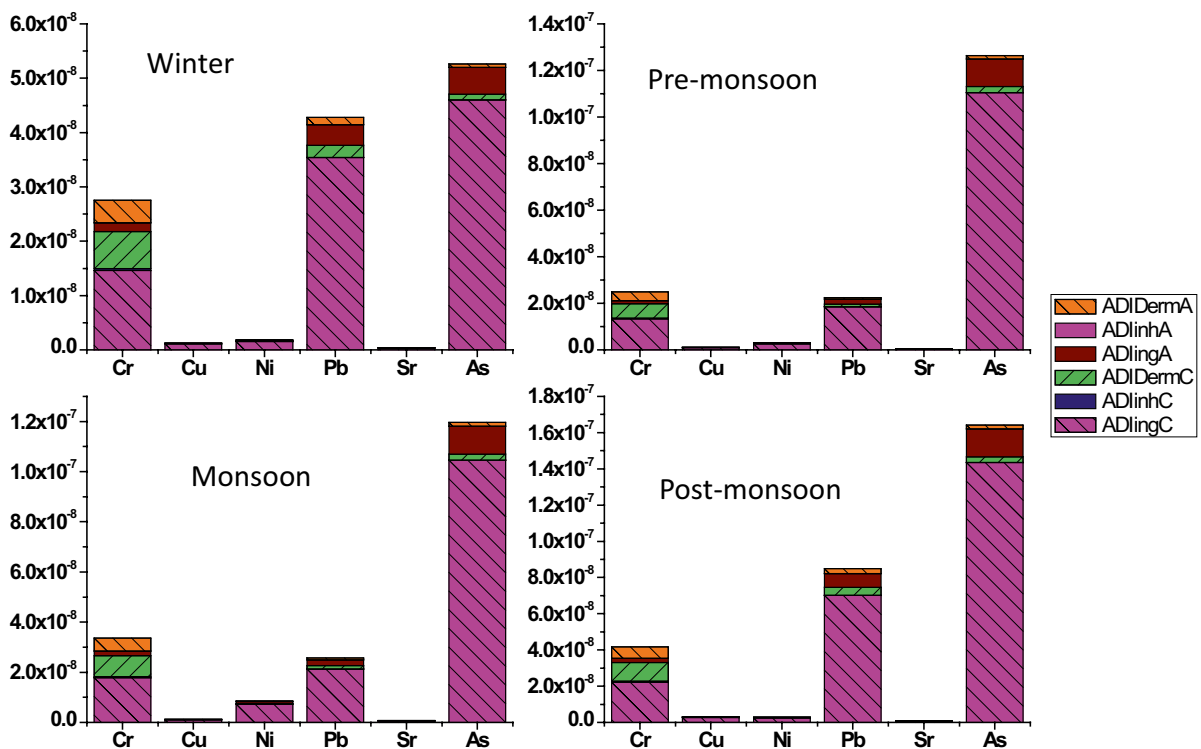


Fig. 13 Non-carcinogenic risk assessment of the selected metal components during different seasons in the same sequence as shown in Fig. 12

compounds), needs to be considered for the overall calculation.

Non-carcinogenic health risk

Apart from the carcinogenic risk hazard quotient (HQ) and hazard index (HI), which have been designed to assess the non-carcinogenic health risk due to heavy metal exposure. The HQ has been obtained by taking the ratio between average daily intake (ADI) to a specific reference dose (RfD).

$$HQ = ADI/RfD$$

The RfD values used for the specific heavy metal have been given in Table 6. RfD is the maximum permissible risk on human beings through daily exposure, specifically considered for sensitive groups during their lifetime (Izhar et al., 2016). An HQ less than 1 can be inferred to mean that there are no adversarial impacts on human health, whereas the average daily dose greater than 1 indicates the harmful effect of the exposure pathway (Zheng et al., 2010). The reference dose values used in this study have also been adopted by many of the previous researchers for health risk assessment caused by ambient air pollution (Kong et al., 2012; Li et al., 2013; Du et al., 2013). The observed trend for HQ for all metals in the sampling site is found to be $HQ_{ing} > HQ_{der} > HQ_{inh}$ for both adult and children. The HI of a contaminant is calculated by adding the HQ values gained for individual metals from all the three exposure pathways (Zheng et al., 2010).

$$HI = \sum (HQ) = HQ_{ing} + HQ_{inh} + HQ_{derm}$$

An HI less than 1 signifies that there is no potential non-carcinogenic risk, which most likely increases as the HI reaches to a value greater than or equal to 1 (Zheng et al., 2010). The values for the non-carcinogenic effects of the measured elements at the sampling site have been summarized in Fig. 13. The observed health risk values less than 1 indicate that the non-carcinogenic risks are well below the standard limit.

Conclusion

PM₁₀ mass over Bhubaneswar (July 2012–August 2013) was characterized in order to understand the variation, potential source contribution, and health risk assessment of the same. A seasonal variation in PM₁₀ mass was observed with a winter maximum, followed by post-monsoon, pre-monsoon, and monsoon

over Bhubaneswar. The percent contribution of average metal concentrations showed an opposite trend than the seasonal variation of the total PM₁₀ mass. The overall metal contribution was highest in monsoon and lowest in winter months. The presence of different metallic components was further confirmed in the PM₁₀ mass through microstructural analysis using FESEM and TEM. There is a substantial evidence that several factors, such as meteorology, pathway traversed by the wind plume, time spent by the trajectory over land, and ocean, influence the total average metal concentrations throughout the year. The enrichment factor also helped to link the source of various metals to either crustal or non-crustal origin, while the PCA revealed three major sources, including crustal and construction, vehicular exhaust/non-exhaust, and industries, as potential contributors to the metals in PM₁₀ mass. The FLEXPART model output revealed that in all of the sampling days, the highest PES values were observed near the sampling site, indicating the consistent effect of regional emissions on the air quality of Bhubaneswar. This study shows that the metal contaminants have the maximum adverse effects on human health when ingested, followed by dermal contact and inhalation pathway. In addition, children are more susceptible to the harmful health effects of metals than adults. Overall, it was concluded that exposure to heavy metals was well below the non-carcinogenic standards; however, the impact of long-term exposure has to be investigated for future action.

Acknowledgements The authors are thankful to the Director, CSIR-IMMT, and the Head, Environment and Sustainability Department, CSIR-IMMT, for their encouragement. TD and BR are grateful to ISRO-GBP (ARFI and ATCTM) and UP is thankful to CSIR for financial support. District Industries Centre, (DIC) Bhubaneswar is highly acknowledged for providing detail about industrial information of Mancheswar industrial estate. All the authors are grateful to the anonymous reviewers for their suggestions to improve the manuscript to a great deal.

Data availability The datasets generated and/or analyzed during the study are available from the corresponding author on reasonable request.

References

- Bhuyan, P., Deka, P., Prakash, A., Balachandran, S., & Hoque, R. R. (2018). Chemical characterization and source apportionment of aerosol over mid Brahmaputra Valley, India. *Environmental Pollution*, 234, 997–1010.

- Calzolari, G., Nava, S., Lucarelli, F., Chiari, M., Giannoni, M., Becagli, S., Traversi, R., Marconi, M., Frosini, D., Severi, M., Udisti, R., et al. (2015). Characterization of PM₁₀ sources in the central Mediterranean. *Atmospheric Chemistry Physics*, *15*, 13939–13955.
- Chantara, S. (2012). PM₁₀ and its chemical composition: a case study in Chiang Mai, Thailand. *Air Quality - Monitoring and Modeling*. (Eds.), ISBN: 978-953-51-0161-1, InTech.
- Das, N., Das, R., Das, S. N., Swamy, Y. V., Chaudhury, G. R., & Baral, S. S. (2011). Comparative studies of chemical composition of particulate matter between sea and remote location of eastern part of India. *Atmospheric Research*, *99*, 337–343.
- Devi, N. L., Kumar, A., & Yadav, I. C. (2020). PM10 and PM2.5 in Indo-Gangetic Plain (IGP) of India: Chemical characterization, source analysis, and transport pathways. *Urban Climate*, *33*, 100663. <https://doi.org/10.1016/j.uclim.2020.100663>
- Du, Y., Gao, B., Zhou, H., Ju, X., Hao, H., & Yin, S. (2013). Health risk assessment of heavy metals in road dusts in urban parks of Beijing, China. *Procedia Environmental Sciences*, *18*, 299–309.
- Duong, T. T., & Lee, B. K. (2011). Determining contamination level of heavy metals in road dust from busy traffic areas with different characteristics. *Journal of Environmental Management*, *92*, 554–562.
- Fang, W., Yang, Y., & Xu, Z. (2013). PM₁₀ and PM_{2.5} and health risk assessment for heavy metals in a typical factory for cathode ray tube television recycling. *Environmental Science & Technology*, *47*, 12469–12476.
- Fassel, V. A. (1977). Current and potential applications of inductively coupled plasma (ICP)-atomic emission spectroscopy (AES) in the exploration, mining, and processing of materials. *Pure and Applied Chemistry*, 1533–1545.
- Furusjo, E., Sternbeck, J., & Cousins, A. P. (2007). PM₁₀ source characterization at urban and highway roadside locations. *Science of Total Environment*, *387*, 206–219.
- Gadhavi, H. S., Renuka, K., Ravi Kiran, V., Jayaraman, A., Stohl, A., Klimont, Z., & Beig, G. (2015). Evaluation of black carbon emission inventories using a Lagrangian dispersion model – a case study over southern India. *Atmospheric Chemistry Physics*, *15*, 1447–1461.
- García-Aleix, J. R., Delgado-Saborit, J. M., Martín-Verdu, G., Amigo-Descarrega, J. M., & Esteve-Cano, V. (2014). Trends in arsenic levels in PM₁₀ and PM_{2.5} aerosol fractions in an industrialized area. *Environmental Science & Pollution Research*, *21*, 695–703.
- Ghosh, S., Rabha, R., Chowdhury, M., & Padhy, P. K. (2018). Source and chemical species characterization of PM₁₀ and human health risk assessment of semi-urban, urban and industrial areas of West Bengal, India. *Chemosphere*, *207*, 626–636. <https://doi.org/10.1016/j.chemosphere.2018.05.133>
- Gugamsetty, B., Wei, H., Liu, C., Awasthi, A., Hsu, S., Tsai, C., Roam, G., Wu, Y., & Chen, C. (2012). Source characterization and apportionment of PM₁₀, PM_{2.5} and PM_{0.1} by using positive matrix factorization. *Aerosol and Air Quality Research*, *12*, 476–491.
- Gullett, B. K., Linak, W. P., Touati, A., Wasson, S. J., Gatica, S., & King, C. J. (2007). Characterization of air emissions and residual ash from open burning of electronic wastes during simulated rudimentary recycling operations. *Journal of Material Cycles and Waste Management*, *9*, 69–79.
- Habeebullah, T. M. A. (2016). Chemical composition of particulate matters in Makkah – focusing on cations, anions and heavy metals. *Aerosol and Air Quality Research*, *16*, 336–347.
- Heintzenberg, J. (1989). Fine particles in the global troposphere A review. *Tellus B*, *41*(2), 149–160. <https://doi.org/10.1111/j.1600-0889.1989.tb00132.x>
- Hieu, N. T., & Lee, B. Y. (2010). Characterization of particulate matter and metals in the ambient air from a residential area in the largest industrial city in Korea. *Atmospheric Research*, *98*, 526–537.
- Hu, X., Zhang, Y., Ding, Z., Wang, T., Lian, H., Sun, Y., & Wu, J. (2012). Bioaccessibility and health risk of arsenic and heavy metals (Cd, Co, Cr, Cu, Ni, Pb, Zn and Mn) in TSP and PM2.5 in Nanjing, China. *Atmospheric Environment*, *57*, 146–152. <https://doi.org/10.1016/j.atmosenv.2012.04.056>
- Huang, K., Zhuang, G., Lin, Y., Wang, Q., Fu, J. S., Zhang, R., Li, J., Deng, C., & Fu, Q. (2012). Impact of anthropogenic emission on air quality over a megacity revealed from an intensive atmospheric campaign during the Chinese Spring Festival. *Atmospheric Chemistry Physics*, *12*, 11631–11645. <https://doi.org/10.5194/acp-12-11631-2012>
- Huang, K., Zhuang, G., Lin, Y., Wang, Q., Fu, J. S., Fu, Q., Liu, T., & Deng, C. (2013). How to improve the air quality over megacities in China: pollution characterization and source analysis in Shanghai before, during, and after the 2010 World Expo. *Atmospheric Chemistry Physics*, *13*, 5927–5942.
- Izhar, S., Goel, A., Chakraborty, A., & Gupta, T. (2016). Annual trends in occurrence of submicron particles in ambient air and health risk posed by particle bound metals. *Chemosphere*, *146*, 582–590.
- Kang, S., Chen, P., Li, C., Liu, B., & Cong, Z. (2016). Atmospheric aerosol elements over the Inland Tibetan Plateau: concentration, seasonality, and transport. *Aerosol Air Quality Research*, *16*, 789–800.
- Kim, K., Kabir, E., & Kabir, S. (2015). A review on the human health impact of airborne particulate matter. *Environment International*, *74*, 136–143. <https://doi.org/10.1016/j.envint.2014.10.005>
- Kong, S., Lu, B., Ji, Y., Zhao, X., Bai, Z., Xu, Y., & Jiang, H. (2012). Risk assessment of heavy metals in road and soil dusts within PM_{2.5}, PM₁₀ and PM₁₀ fractions in Dongying city, Shandong Province, China. *Journal of Environmental Monitoring*, *14*(3), 791–803.
- Kulshrestha, A., Satsangi, P. G., Masih, J., & Taneja, A. (2009). Metal concentration of PM_{2.5} and PM₁₀ particles and seasonal variations in urban and rural environment of Agra, India. *Science of Total Environment*, *407*, 6196–6204. <https://doi.org/10.1016/j.scitotenv.2009.08.050>
- Li, X., Chen, Z., Chen, Z., & Zhang, Y. (2013). A human health risk assessment of rare earth elements in soil and vegetables from a mining area in Fujian Province, Southeast China. *Chemosphere*, *93* (6), 1240–1246. <https://doi.org/10.1016/j.chemosphere.2013.06.085>
- Li, Z., Hopke, P. K., Husain, L., Qureshi, S., Dutkiewicz, V. A., Schwab, J. J., Drewnick, F., & Demerjian, K. L. (2004). Sources of fine particle composition in New York City. *Atmospheric Environment*, *38*, 6521–6529.

- Lough, G. C., Schauer, J. J., Park, J. S., Shafer, M. M., DeMinter, J. T., & Weinstein, J. P. (2005). Emissions of metals associated with motor vehicle roadways. *Environmental Science & Technology*, *39*, 826–836.
- Mahapatra, P. S., Panda, S., Das, N., Rath, S., & Das, T. (2013). Variation in black carbon mass concentration over an urban site in the eastern coastal plains of the Indian sub-continent. *Theoretical and Applied Climatology*. <https://doi.org/10.1007/s00704-013-0984-z>
- Mahapatra, P. S., Panda, S., Walvekar, P. P., Kumar, R., Das, T., & Gurjar, B. R. (2014). Seasonal trends, meteorological impacts, and associated health risks with atmospheric concentrations of gaseous pollutants at an Indian coastal city. *Environmental Science & Pollution Research*. <https://doi.org/10.1007/s11356-014-3078-2>
- Mahapatra, P. S., Sinha, P. R., Boopathy, R., Das, T., Mohanty, S., Sahu, S. C., & Gurjar, B. R. (2018). Seasonal progression of atmospheric particulate matter over an urban coastal region in peninsular India: role of local meteorology and long-range transport. *Atmospheric Research*, *199*, 145–158.
- Mallik, C., Mahapatra, P. S., Kumar, P., Panda, S., Boopathy, R., Das, T., & Lal, S. (2019). Influence of regional emissions on SO₂ concentrations over Bhubaneswar, a capital city in eastern India downwind of the Indian SO₂ hot-spots. *Atmospheric Environment*, *209*, 220–232. <https://doi.org/10.1016/j.atmosenv.2019.04.006>
- Monika, J. K. (2010). E-waste management: as a challenge to public health in India. *Indian Journal of Community Medicine*, *35*(3), 382–385.
- Nishanth, T., Praseed, K. M., Satheesh, M. K., & Valsaraj, K. T. (2014). Influence of ozone precursors and PM₁₀ on the variation of surface O₃ over Kannur, India. *Atmospheric Research*, *138*, 112–124.
- Ondráček, J., Schwarz, J., Ždímal, V., Andělová, L., Vodička, P., Bizek, V., ... & Smolík, J. (2011). Contribution of the road traffic to air pollution in the Prague city (busy speedway and suburban crossroads). *Atmospheric Environment*, *45*(29), 5090–5100. <https://doi.org/10.1016/j.atmosenv.2011.06.036>
- Panda, S., Sharma, S. K., Mahapatra, P. S., Panda, U., Rath, S., Mahapatra, M., Mandal, T. K., & Das, T. (2016). Organic and elemental carbon in PM_{2,5} over mega city New Delhi and Bhubaneswar, an Eastern Coastal Site in India. *Natural Hazards*, *80*, 1709–1728. <https://doi.org/10.1007/s11069-015-2049-3>
- Panda, U., & Das, T. (2017). Micro-structural analysis of individual aerosol coarse particles during different seasons at an eastern coastal site in India. *Atmospheric Pollution Research*, *8*(1), 196–207.
- Panda, U., Mahapatra, P. S., & Das, T. (2015). Study of C₂–C₅ non-methane hydrocarbons and their ozone formation potential at Bhubaneswar, an Eastern Coastal Site in India. *MAPAN Journal of Metrology Society of India*, *30*, 195–202. <https://doi.org/10.1007/s12647-015-0134-4>
- Park, E. J., Kim, D. S., & Park, K. (2008). Monitoring of ambient particles and heavy metals in a residential area of Seoul, Korea. *Environmental Monitoring Assessment*, *137*, 441–449.
- Pascal, M., Falq, G., Wagner, V., Chatignoux, E., Corso, M., Blanchard, M., Host, S., Pascal, L., & Larriou, S. (2014). Short-term impacts of particulate matter (PM₁₀, PM_{10-2.5}, PM_{2.5}) on mortality in nine French cities. *Atmospheric Environment*, *95*, 175–184.
- Perrino, C., Tiwari, S., Catrambone, M., Torre, S. D., Rantica, E., & Canepari, S. (2011). Chemical characterization of atmospheric PM in Delhi, India, during different periods of the year including Diwali festival. *Atmospheric Pollution Research*, *2*, 418–427.
- Police, S., Sahu, S. K., & Pandit, G. (2016). Chemical characterization of atmospheric particulate matter and their source apportionment at an emerging industrial coastal city, Visakhapatnam, India. *Atmospheric Pollution Research*, *7*, 725–733.
- Saffaripour, M., Thomson, K. A., Smallwood, G. J., & Lobo, P. (2020). A review on the morphological properties of non-volatile particulate matter emissions from aircraft turbine engines. *Journal of Aerosol Science*, *139*, 105467.
- Sax, I. N. (1968). Dangerous properties of industrial materials. New York Reinhold Book Corp.
- Seibert, P., & Frank, A. (2004). Source-receptor matrix calculation with a Lagrangian particle dispersion model in backward mode. *Atmospheric Chemistry Physics*, *4*, 51–63.
- Sharma, S. K., Sharma, A., Saxena, M., Choudhary, N., Masiwal, R., Mandal, T. K., & Sharma, C. (2015). Chemical characterization and source apportionment of aerosol at an urban area of Central Delhi, India. *Atmospheric Pollution Research*, *1*–12.
- Singh, U. K., & Kumar, B. (2017). Pathways of heavy metals contamination and associated human health risk in Ajay River basin, India. *Chemosphere*, *174*, 183–199.
- Sivaramanan, S. (2013). E-waste management, disposal and its impacts on the environment. Universal. *Journal of Environmental Research and Technology*. *3*(5), 531–537.
- Song, F., & Gao, Y. (2011). Size distributions of trace elements associated with ambient particular matter in the affinity of a major highway in the New Jersey New York metropolitan area. *Atmospheric Environment*, *45*, 6714–6723.
- South Asia Environment Outlook 2014. (2014). <http://www.sacep.org/pdf/Reports-Technical/2014-South-Asia-Environment-Outlook-2014.pdf>
- Stohl, A., Hittenberger, M., & Wotawa, G. (1998). Validation of the lagrangian particle dispersion model FLEXPART against large scale tracer experiment data. *Atmospheric Environment*, *32*, 4245–4264. [https://doi.org/10.1016/s1352-2310\(98\)00184-8](https://doi.org/10.1016/s1352-2310(98)00184-8)
- Sudheer, A. K., & Rengarajan, R. (2012). Atmospheric mineral dust and trace metals over urban environment in western India during winter. *Aerosol Air Quality Research*, *12*, 923–933. <https://doi.org/10.4209/aaqr.2011.12.0237>
- Tao, Y., Mi, S., Zhou, S., Wang, S., & Xie, X. (2014). Air pollution and hospital admissions for respiratory diseases in Lanzhou, China. *Environmental Pollution*, *185*, 196–201.
- Turley, C. D., Brenchley, D. L., & Landolt, R. R. (2012). Barium additives as diesel smoke suppressants. *Journal of the Air & Waste Management Association*, *23*(9), 783–787.
- US Environmental Protection Agency. (1989). Risk Assessment Guidance for Superfund Volume 1: Human Health Evaluation Manual (Part A); Office of Emergency and Remedial Response: Washington, DC, USA.
- USEPA. (1998). Methods 3051a microwave assisted acid digestion of sediments, sludge, soils and oils. <http://www.gov/SW-846/pdfs/3051a.pdf>

- USEPA. (2007). Framework for Metals Risk Assessment. Office of the Science Advisor: Washington, DC, EPA 120/R-07/001.
- U.S. EPA (U.S. Environmental Protection Agency). (2009). Risk Assessment Guidance for Superfund Volume I: Human Health Evaluation Manual (Part F, Supplemental Guidance for Inhalation Risk Assessment). Office of Superfund Remediation and Technology Innovation, Washington, D.C.
- Wedepohl, K. H. (1995). The composition of the continental crust. *Geochimica et Cosmochimica Acta*, 59, 1217–1232.
- Wendt, R. H., & Fassel, V. A. (1965). Induction-coupled plasma spectrometric excitation source. *Analytical Chemistry*, 37, 920–922.
- World Health Organization. (2006). *Air quality guidelines, Global update 2005, Particulate matter, ozone, nitrogen dioxide and sulfur dioxide*. World Health Organization.
- Zheng, N., Liu, J., Wang, Q., & Liang, Z. (2010). Health risk assessment of heavy metal exposure to street dust in the zinc smelting district, Northeast of China. *Science of the Total Environment*, 408(4), 726–733. <https://doi.org/10.1016/j.scitotenv.2009.10.075>

Publisher's Note Springer Nature remains neutral with regard to jurisdictional claims in published maps and institutional affiliations.